Evidence for a Recent Formation of the Isthmus of Panama 0.6 Mya

Leonidas Brikiatis (lb@aegeanman.com)
Unaffiliated

Research Article

Keywords: Isthmus , Panama , oceanographic, climatic, biogeographic, evolutionary hypotheses

Posted Date: July 7th, 2021

DOI: https://doi.org/10.21203/rs.3.rs-604885/v1

Abstract

The exact age of the final formation of the Isthmus of Panama is a critical reference point for oceanographic, climatic, biogeographic, and evolutionary hypotheses. Geotectonic evidence suggests that the isthmus was completed between 12 Mya and 3 Mya, and an age of 3–4 Mya has been used as a benchmark in hundreds of studies over the past 30 years. Phylogeographic data indicate the existence of marine connections across the isthmus much more recently, however. I reconsider the available geotectonic, biostratigraphic, oceanographic, and paleoclimatic data and show that multiple lines of indirect evidence suggest that four transisthmian seaways may have persisted until as recently as the onset of the Middle Pleistocene (~ 0.6 Mya). Subduction of the Cocos Plate beneath one transisthmian seaway (the only seaway featuring a deep sill) caused rapid tectonic shoaling and reorganisation of oceanic currents, which coincided with a major glacioeustatic sea level fall ~ 950–917 Mya that led to a temporary closing of the Bering Strait. This resulted in unusual and contrasting climate phenomena, including the "900-Kyr (cold) event" and the "greening" of South Greenland during the MIS 22 glacial maximum. The concurrence of the final formation of the Isthmus of Panama with the mid-Pleistocene Transition of glacial/interglacial periodicity suggests a tight relationship between these events.

1. Introduction

The final formation of the Isthmus of Panama is one of the most significant events in the recent geological history of the Earth[1,2,3], because it resulted in the closure of the Central American Seaway (CAS), which along with its precursor the Hispanic Corridor, connected the Pacific and Atlantic Oceans since the Late Jurassic (160 Mya)[4,5] (Fig. 1A). Different ages have been proposed for the event, including the very ancient Miocene (23 Mya[1] or 14 Mya[6]) and the more recent Late Pliocene (3.5 Mya or 2.8 Mya[7,8]). Some authors have questioned these dates by highlighting the persistence in more recent times of narrow and shallow seaways connecting the Atlantic and Pacific (e.g. ref.[2]), whereas others point to marine paleontological evidence indicating shallow-water faunal exchanges from the Early Pleistocene (Gelasian) until about 2–1.8 Mya[9,10]. Although the various proposed ages probably correspond to distinct ephemeral exposures[1], the most recent and final exposure is the most important, because it modulated the modern oceanographic, climatic, and biogeographic configuration of the Earth. By influencing the Gulf Stream intensity and, in turn, the configuration of the Atlantic meridional overturning circulation (AMOC), the final formation of the isthmus modulated the modern European and global climates [ref.[11,12] and references therein]. Moreover, the operation of the isthmus as a barrier to marine dispersals and a corridor for terrestrial dispersals affected the diversity and geographic distributions of the biota of North and South America[1,2,13]. Therefore, the age and regime of the final formation of the Isthmus of Panama have important implications to oceanographic and climatic models, biogeographic hypothesis, and the calibration of evolutionary rates[1,2,3]. For example, in the absence of relevant paleontological records, hundreds of molecular dating studies of transisthmian "geminate" species have calibrated their molecular clocks using a ~ 3–4 Mya age of the final formation of the Isthmus of Panama as a benchmark[1,2]. This age is widely accepted at present and is based on interpretation of the available

geological evidence, which is summarised in the Late Pliocene (3 Mya) palaeogeographical reconstruction of Coates and Obando[8] (Fig. 1C) and reproduced in more recent biogeographical analyses (e.g. ref.[14]).

Here, I review the available geological, biostratigraphic, oceanographic, and paleoclimatic data and show that multiple sources of evidence suggest that the complete and final closure of the Isthmus of Panama occurred much more recently than was previously believed.

2. Materials And Methods

The formation of the Isthmus of Panama can be tracked through the signatures that it left on the surrounding biotic and abiotic environment and, more generally, on the biosphere. Current beliefs about the age of the final formation of the isthmus are mainly based on interpretation of geological evidence, which is not sufficient to reconstruct the palaeogeographical history of the area, given the difficulty of making direct geological observations and the fact that much of the geological record is eroded as a result of the complex geological history of the area[61]. Although biogeographical information can be useful in palaeogeography and has often been invoked in the past (e.g. ref.[62]), previous efforts to determine the palaeogeography of the Isthmus of Panama (e.g. ref.[1]) did not manage to separate a clear and detailed biogeographical signal. Here, I use all of the available phylogeographical information to infer a specific palaeogeographical scenario suggested by the data. I then consider the congruence between this scenario and the available geotectonic, biostratigraphic, oceanographic, and paleoclimatic data. Regarding the latter, I investigate whether the formation of the Isthmus of Panama is related to the occurrence of the great paleoclimatic change known as the MPT.

2.1. Phylogeographic data

Molecular divergence dates of transisthmian geminate species and populations have been widely used to infer conclusions regarding the formation of the Isthmus of Panama (e.g. ref.[1]). Such divergence dates can be considered reliable only if they are calibrated on independent calibration points rather than on a benchmark date for the formation of the isthmus, because the a priori assumption of a benchmark date for the formation of the isthmus leads to circularity if the goal is to examine the timing of dispersal or vicariance across the isthmus[1]. On the other hand, the characterisation of species or populations as “geminate” is itself subject to limitations and uncertainties, which can influence the phylogeographic conclusions[37]. A proper selection of geminate species should make clear how the invoked speciation is related to the formation of the isthmus, because different forms of life have different capabilities to overpass specific biogeographical barriers, so their biogeographical significance in paleogeographic reconstructions varies accordingly.

In the present work, I categorise the phylogeographical data by qualitatively evaluating its importance and clarity regarding the general concept of a recent isthmus formation as well as the exposure of specific transisthmian seaways. The formation of the Isthmus of Panama is assumed to have

predominantly caused vicariant speciation of marine biota and terrestrial biota that dwell exclusively in coastal areas and are unable to cross inland features such as hills, mountains, and forests. Geminate coastal species of this category (Category A) are currently distributed on either side (Atlantic and Pacific) of the isthmus, because the inland of the isthmus developed a physical barrier to interbreeding between Atlantic and Pacific populations of the common ancestor and thus led to vicariant speciation (see the graphical example in **Supplementary Fig. 1**).

Squirrel monkeys (genus *Saimiri*) currently inhabit each of the areas of vertebrate endemism in the Amazon (i.e. the Atlantic side of South America), but one species, *Saimiri oerstedii*, exists only in a small coastal area on the Pacific side of Central America[42]. The restricted distribution of *S. oerstedii* is accredited to specialisation to a lowland coastal niche, which is thought to have been a characteristic of the last common ancestor of *S. oerstedii* and the other *Saimiri* species[42]. The divergence between *S. oerstedii* and *Saimiri sciureus*, which is found in the northern Amazon, is estimated to have occurred ~ 0.95 Mya[42]. Sea birds are another example of coastal organisms for which inland areas present a barrier[63]. The most recent common ancestor of regional populations of masked boobies (*Sula dactylatra*) on either side of the Isthmus of Panama is estimated to have lived ~ 0.64 Mya[43].

Mangrove coastal vegetation is often considered to harbour the signatures of historical vicariance events[64]. It has been argued that because mangrove or coastal habitats were the last to disappear during the final closure of the CAS, the species that inhabited those environments were probably the last to be separated by the closure event[65] (**Supplementary Fig. 1**). Therefore, the divergence times of mangrove species should correspond accurately to the final completion of the isthmus[65]. The Pacific and Atlantic populations of the black mangrove (*Avicennia germinans*) are estimated to have evolved independently since ~ 0.84 Mya[44]. Equivalent divergence dates have been reported for the mangrove-inhabiting fishes of the transisthmian genera *Dormitator*[33], *Anisotremus*[1], and *Mulloidichthys*[1] (**Table 1**).

Table 1. Molecular divergence dates of coastal transisthmian geminate species and populations.

	Type of Life Form	Pacific Coast Variety	Atlantic Coast Variety	Divergence Time (Mya)	Calibration	Reference
1	Fishes	*Mulloidichthys dentatus*	*Mulloidichthys martinicus*	0.65	Standard molecular clock rate	1
2	Fishes	*Abudefduf concolor*	*Abudefduf taurus*	0.7	Standard molecular clock rate	1
3	Fishes	*Anisotremus interruptus*	*Anisotremus surinamensis*	0.8-1.12	1. Standard molecular clock rate; 2. plus fossils	1
4	Fishes	*Dormitator latifrons*	*Dormitator sp.*	0.98	Fossils	33
5	Fishes	*Anchoa delicatissima*	*Anchoa parva*	0.4-0.75	fossils	34 (0.75); 35 (0.4)
6	Fishes	Pacific species lineage of *Old World Anchovies (genus Engraulis)*	Atlantic species lineage of Old World Anchovies (genus *Engraulis*)	0.67	Mainly on fossils	35
7	Fishes	*Lycengraulis poeyi*	*Lycengraulis grossidens*	0.88	Combined, on two fossils and a Panama closure date	35
8	Decapoda/Shrimps	*Banded coral shrimp, Stenopus hispidus*	Banded coral shrimp, *Stenopus hispidus*	1.09	On updated decapode divergence rate	36
9	Decapoda/Crabs	*Eurytium tristani*	*Eurytium occidentalis*	0.63	Date of Messinian Salinity Crisis	37
10	Arthropoda/Marine littoral springtails	*Psammisotoma dispar*	*Psammisotoma dispar*	1.04	Standard mutation rate	38
11	Marine Bivalves/Deep-sea clums	*Abyssogena novacula+mariana*	*Abyssogena southwardae*	0.95	Fossils	39
13	Marine Bivalves/Deep-sea mussels	Species lineage of *Bathymodiolus thermophilus*	Species lineage of *Bathymodiolus azoricus, B. puteoserpentis* and *B. heckerae*	1.1	Assuming that rates across sites vary according to a discretized gamma distribution	40
14	Mammals/Cetaceans	Fin Whales (*Balaenoptera physalus spp.*)	Fin Whales (Balaenoptera physalus spp.)	0.95-0.99	On fossil-based divergence date	41
15	Mammals/Primates	*Saimiri oerstedii*	*Saimiri saimiri sciureus*	0.77-0.95	Fossils-based *Saimiri* crown age	1 (0.77); 42 (0.95)
16	Birds/Seabirds	*Sula dactylatra*	*Sula dactylatra*	0.64	Standard "bird mutation rate"	43
17	Plants	Mangrove *Avicennia germinans*	Mangrove *Avicennia germinans*	0.84	Standard mutation rate	44

With regards to marine biota vicariance, there are several shallow-water fishes, decapoda, arthropods, and bivalves dwelling on either side of the isthmus whose divergence times have been dated close to, or since, 1 Mya using independently calibrated molecular clocks (**Table 1**). Most of these species are inhabitants of mangrove environments, suggesting a shallow-water property in the last transisthmian seaways. However, the existence of some deep-water species in Category A suggest that at least one of the seaways maintained a deep sill.

In addition to the examples in Category A, there are many other potential geminate species with molecular divergence dates that are comparable with a < 1 Mya age of the formation of the Isthmus of Panama, including plants, insects, reptiles, and birds (e.g. Supplementary Table 8 in ref.[1]). Invocation of these species as direct evidence of the age of the formation of the isthmus would require composite dispersal scenarios with a substantial degree of uncertainty, however, so they are counted here as indirect evidence. The most significant of them have been included in a separate Category (Category B) that includes species with distinct (Category B1; **Supplementary Table 1**) or overlapping (Category B2; **Supplementary Table 2**) distributions on both sides of the proposed former transisthmian seaways.

Detailed palaeogeographical information about the exposures of the transisthmian seaways in specific locations can be extracted from the phylogeography of terrestrial species with limited dispersal, that is, species (mainly endemic) that inhabit the same area for a long time. Accordingly, one can suppose that genetically distinct populations that today inhabit regions on both sides of former seaways will have molecular divergence dates that correspond to the last exposure of the seaways. Species in this category include freshwater dwellers such as fishes and frogs (**Supplementary Table 3 and Supplementary Appendix**). For example, genetic variants of the freshwater catfish *Pimelodella chagresi* with an estimated divergence time ~ 0.9 Mya[66] are currently distributed on either side of the ancient locations of the Barú, Canal, and Atrato Seaways (see **Supplementary Appendix**). In addition, genetic variants of the mosquito *A. albimanus*[67] can be used to help reconstruct the positions of the Early Pleistocene seaways just before the final formation of the Isthmus of Panama. The rationale for that approach is that as the relative sea level fell during the formation of the isthmus, saltwater swamps with mangrove vegetation would have developed in the emergent lowlands that were previously occupied by seaways, creating favourable conditions for the saline-tolerant *A. albimanus* to disperse across the isthmus. *A. albimanus* is one of the approximately 5% of mosquito species that live in either brackish or saline water, having adapted a highly developed system to regulate salinity[68]. The continuing sea level fall finally dried the saltwater swamps and separated the ancestral population of *A. albimanus* into isolated regions.

2.2. Geotectonic data

The hypothesis that the final formation of the Isthmus of Panama occurred ~ 3 Mya is summarized in the latest Neogene-Quaternary palaeogeographical reconstructions of Coates and Obando[8] (Fig. 1B & 1C). According to that scenario[8], interoceanic marine communication through the isthmus was maintained until the Pliocene via three persistent seaways (Fig. 1C): the Nicaraguan Seaway (through the Nicaragua Depression), the Canal Seaway (through the area of the current Panama Canal), and the Atrato Seaway (through the Atrato Basin of Colombia) (see also ref.[69]). Another seaway, here called the Barú Seaway, although shown in Coates and Obando's Late Miocene (~ 6 Mya) palaeogeographical reconstruction (Fig. 1B), was considered to be subaerially exposed in their 3 Mya reconstruction (Fig. 1C). In the following sections, I review the available geotectonic data in order to determine whether recent developments in geoscience support this palaeogeographical scenario.

2.2.1. The Nicaraguan Seaway

The Nicaraguan Depression is a prominent, 40–70 km wide tectonic graben extending ~ 1000 km from the Caribbean side of Costa Rica in the southeast to the northern Gulf of Fonseca in El Salvador (Figs. 2 & 3). The depression has been interpreted as having probably developed since the Pliocene[70,71]. The most recent structural studies of the El Salvador Fault Zone show that the graben structures are the result of a two-phase evolution starting with an initial extensional phase that occurred between 7.2–6.1 Mya (latest Miocene) and 1.9–0.8 Mya (Early Pleistocene)[72]. At the northwest side of the Nicaraguan Seaway (sensu Coates and Obando[8]), the shallow-water El Salto Formation unconformably overlies older sequences (the

Rivas, Brito, Masachapa, and El Fraile Formations) of various ages from Cretaceous to Pliocene[71]. While the fossil sites in Nicaragua have so far produced only land mammals of Late Pleistocene age, a baleen whale was found in the Mine K-11 locality within the El Salto Formation[73]. Pyroclastic-alluvial deposits of the Las Sierras Group succeed the marine deposits of the El Salto Formation, so the age of the El Salto deposition corresponds to the minimum age of the Nicaraguan Seaway at its northwest end. Based on molluscan fossil findings, an Early Pliocene age has long been assigned to the El Salto Formation; however, that age is considered to be poorly constrained (ref.[73] and references therein). Correlation of offshore commercial wells in the Sandino basin and onshore stratigraphic studies showed[74] that although the El Salto Formation includes the complete Pliocene, its top (sequence 12, SB12) reaches up to the early-to-mid Pleistocene Transition ~ 0.9 Mya. This age is congruent with the end of the second, transtensional phase of the formation of the Nicaraguan Depression (1.9–0.8 Ma; Early Pleistocene), implying that the associated extensional structures are contemporaneous with, and might have led to, the deposition of the El Salto Formation, which has a thickness of 100 m onshore and up to 1,000 m offshore.

The two large freshwater lakes, Lake Nicaragua and Lake Managua, contained in the Nicaraguan Depression are also considered to have been formatted since the Early Pleistocene[75]. Investigations of whether and when the lakes were last connected to the oceans did not reach a clear conclusion[76]. Nevertheless, the occurrence of marine-like nematodes such as *Theristus setosus* (Btitschli) Filipjev (an inhabitant of marine and brackish environments[77]), *Polygastrophora octobulba* (an inhabitant of marine and freshwater environments[78]), and the endemic *Viscosia nicaraguensis* (considered to originate from the marine *Viscosia papillate*[79]) in the lakes does not exclude the possibility that the lakes were once connected directly to the sea (ref.[76] and references therein).

In any case, Coates and Obando[8] independently showed that the Pacific seashore reached at least the middle of the Nicaraguan Seaway (Venado Formation, San Carlos Basin) during the Early Pleistocene (see also ref.[80]) and maybe had a southward connection via the Tempisque Basin as well (see map in ref.[14,81]). They further suggested that thereafter, during the Pliocene, the Nicaraguan Seaway was connected (although somehow restricted by the Sarapiquí Arch) to the Caribbean Sea through the Northern Limón Basin.

The Northern Limón Basin is an undeformed, normal faulted back arc basin that is separated from the Southern Limón Basin by the Moín High, and from the San Carlos Basin to the west by the Sarapiquí Arch[80]. Miocene regional uplifting of the inner arc formed a series of intermountain basins on the western, inland portion and shallow marine conditions on the eastern, Caribbean side. Subsequently, prograded fan deltaic, continental fan deposits, and patch reef development produced bay conditions corresponding to the Plio-Pleistocene Suretka Formation[80]. Such a transition is displayed in the classic stratigraphic scheme of the Limón Basin,[82] where the Middle Miocene–Early Pliocene, deltaic shallow marine Río Banano Formation is unconformably succeeded by the shallow marine and continental rocks

of the Plio-Pleistocene Suretka Formation (e.g. ref.[83] and references therein). According to this very generalised stratigraphical interpretation, the conglomerates of the Suretka Formation demonstrate the southwards exposure limit of the Nicaraguan Seaway toward the Atlantic. This view is reproduced in the palaeogeographical reconstruction of Coates and Obando,[8] which is based on a 2.5 Mya estimation for the age of the upper boundary of the Río Banano Formation[84]. That age cannot be assumed for the younger marine depositions in the Northern Limón Basin, however, because it is based entirely on cross-section data from the Southern Limón Basin,[84] which experienced a different geodynamic history and deformation than the Northern Limón Basin and is much more poorly studied[80,83]. For example, although the Northern Limón and San Carlos Basins cover a 12.000 km^2 onshore area, only three deep wells have been drilled on land,[80] and outcrops are extremely rare[85]. On the other hand, the age of the Suretka Formation is unapproved, as no index fossil that dates a geological age was ever found[86]. Therefore, the stratigraphical data from the Southern Limón Basin are not representative of the palaeogeography of the Northern Limón Basin.

Recent geological research based on well and seismographic analyses showed that continuous marine Pleistocene deposits can be laterally traced for several tens of kilometres on the northwest-to-southeast coastline northwards of the Moín High[83,87] and across the whole coast of the Northern Limón Basin (see ref. [80]: Fig. 10). Therefore, given the potential for extended Pleistocene deposits in the Northern Limón Basin, the most recent age corresponding to the complete transoceanic exposure of the Nicaraguan Seaway is not defined by the conglomerates of the Suretka Formation, but instead by the Early Pleistocene deposits of the Venado Formation in the San Carlos Basin. Today, only 34 m of relief separates Caribbean and Pacific waters in the area of the San Carlos basin[88], and it is likely that the area has been slightly uplifted under the tectonic effect of the Cocos Ridge subduction beneath Costa Rica during the Early Pleistocene.

2.2.2. The Barú Seaway

In the Late Miocene (~ 6 Mya) palaeogeographical reconstruction of Coates and Obando[8] (Fig. 1B), the Atlantic Bocas del Toro Basin and the Pacific Burica Basin are connected by a marine trough, which I refer to as the Barú Seaway because of its location where the Barú volcano (3,474m) is today (Figs. 2 & 3). Also in the vicinity of the Barú Seaway is the Panama Fracture Zone, an active right lateral-moving transform fault that forms part of the tectonic boundary between the Cocos and Nazca Plates and the larger southeast-moving triple junction between the Cocos, Nazca, and Caribbean Plates[89]. As the oceanic crust of the Cocos Plate moved north eastward, it was partially subducted beneath the volcanic arc system of Costa Rica and western Panama, causing rapid elevation of the Central American Isthmus from the Arenal volcano in Costa Rica to El Valle in Panama. The result of this orogenic procedure is the mountain range of Cordillera de Talamanca (eastern Costa Rica) and Cordillera Central (western Panama)[89,90], which cuts off the Barú Seaway and other interoceanic basins across the isthmus in the Late Pliocene (~ 3 Mya) reconstruction of Coates and Obando[8], supporting the view of a complete formation of the Isthmus of Panama around the same time as the rise of the mountain range. Therefore,

the exact age of the orogenic uplift due to the Cocos Plate collision is fundamental to scenarios of the final formation of the Isthmus of Panama.

The timing of Cocos Ridge subduction is currently one of the most widely discussed debates in Central American tectonics,[91,92] with estimates ranging from as old as 8 Ma (e.g. ref.[93]) to as young as 0.5 Ma (e.g. ref.[94]). The youngest estimates for the Cocos Ridge arrival (0.5–3.5 Ma) at the Middle America Trench are derived from onshore rock uplift and subsidence patterns as well as plate reconstructions, whereas the oldest estimates (8–5 Ma) are largely based on the cessation of “normal” (non-adakitic) calc-alkaline volcanism within the Cordillera de Talamanca (ref.[91] and references therein). Recent studies have concluded that the cessation of arc volcanism and the onset of Cocos Ridge collision (< 3 Ma) are separate events, however, reflecting recent changes in the configuration of the plate boundary system[91,92]. Hence, scenarios for a young age of Cocos Ridge subduction are increasingly favoured today.

Deposition facies of the Burica Peninsula on the Pacific side of the isthmus have been studied as a proxy for the tectonic movements of the Cocos Plate, because the peninsula is located at the eastern edge and front of the plate. The facies nomenclature used here is based on ref.[95]. The most comprehensive study of the area[29] concluded that the marine faunal evidence contained in the Pliocene to Early Pleistocene (3.5–1.5 Mya) Burica Member of the Charco Azul Formation suggests strong subsidence and a bathyal environment (~ 2,000 m) in the area during the Early Pliocene, followed by gradual shoaling from 2,000 m to 1,400 m during the Late Pliocene through Early Pleistocene. Overlain strata assigned to the lowermost Armuelles Formation (late Early Pleistocene) were found to contain faunas indicative of water depths between 1,200 m and 1,300 m. By contrast, shallow-water molluscs in stratigraphically higher exposures of the Armuelles Formation are indicative of shelf deposits. Therefore, within the deposition interval of the Armuelles Formation, rapid shoaling took place at a time corresponding to the “Early Pleistocene–Late Pleistocene boundary”. These findings led Corrigan et al.[29] to conclude that rapid uplift due to Cocos Plate subduction took place after the Early Pleistocene. In agreement with that view, Gardner et al.,[94] using a radiometrically calibrated geodynamical model, concluded that the collision took place 0.5 Mya.

In contrast to these views, Collins et al.[90] considered the whole Armuelles Formation to include very shallow-water deposits (< 10 m) and proposed that the rapid 2,000 m uplift in the Burica Peninsula falls within the interval of deposition of the underlain Burica Member of the Charco Azul Formation from the Late Pliocene. Furthermore, Collins et al.[90] suggested that the subduction of the buoyant Cocos Ridge and the orogeny of the Cordillera de Talamanca began about 3.6 Ma, or 2 to 3 million years earlier than the date proposed by Corrigan et al.[29] and Gardner et al.[94]. In particular, based on a ~ 1.6 Ma age for the top of the Moín Formation (i.e. the age of the most recent marine deposits in the Southern Limón Basin at the Atlantic coast to the north), Collins et al.[90] concluded that the subaerial exposure of the Southern Limón Basin was caused by uplift from the delivery of the subducted Cocos Plate. Therefore, they placed the whole orogenesis within the interval 3.6–1.6 Mya. However, subsequent studies of the Southern Limón Basin revised the age of the basin uplift to < 1 Ma[96], and more recent studies concluded that the

whole Colón carbonate platform in the Bocas del Toro region of Panama (south of the Southern Limón Basin) was finally subaerially exposed during a Middle Pleistocene regional uplift[97]. Geological research in the Bocas del Toro region of Panama found that although neritic deposits persisted in the Northern region (Colón platform) until the end of the Early Pleistocene, there was a hiatus in deposition over a distance of ~ 80 km between Isla Colón and the Escudo de Veraguas Island (yellow line in Fig. 3) during the last 3.5 Myr and over an even greater distance within the last 1.8 Mya[98]. Therefore, the available data are not sufficient to refute the existence of a seaway with bathyal property during the hiatus interval.

In the middle of the proposed Barú Seaway, where the Barú volcano (3,474 m) stands today, there is independent evidence that low-elevation relief (< 500 m) may have persisted until as recently as the mid-Pleistocene, whereas rapid uplift took place thereafter[21]. Moreover, the age of the Barú volcano formation is considered to be ~ 0.5 My. It is therefore likely that the uplift that closed the Barú Seaway was a recent event that took place around the Early to Middle Pleistocene boundary (1–0.5 Mya). Indeed, most recent geotectonic analyses are congruent with the palaeobythometric interpretation of Corrigan et al.[29] rather than the interpretation of Collins et al.[90] (e.g. ref.[92,95]), suggesting that neither the Osa Peninsula nor the Burica Peninsula was emergent until at least 1 Ma, when the axis of the Cocos Ridge reached the Middle American Trench[92].

2.2.3. The Canal Seaway

The Canal Basin (in a broad sense) is an elongate, northwest-southeast–trending transisthmian sedimentary trough controlled by a fault system known as the Canal Discontinuity,[99] which extends across the isthmus within an 80-km wide zone (Figs. 2 & 3). Today, it results in a major topographic discontinuity between high volcanic mountain ranges to the east and west and lowlands punctuated by small (generally < 300 m high) topographic features of unclear tectonic and/or volcanic origins[100]. It remains uncertain whether the topographic highs in the Canal Basin are erosional remnants of ancient volcanic landforms that could have obstructed an interoceanic strait or instead of islands within a more recent interoceanic seaway[101].

In the simplest terms, the geology of the Canal Basin consists of a pre-middle Eocene volcanic basement overlain by late Eocene to Late Miocene marine deposits interbedded with volcanic and volcaniclastic rocks[102]. Younger deposits are generally poorly exposed. The relatively recent scenario for the formation of the Isthmus of Panama depicted in the Pliocene palaeogeographical reconstruction of Coates and Obando[8] is based on the assumption of a Pliocene age for the most recent marine deposits in the Canal Basin (i.e. those at the top of the Chagres Sandstone; e.g. ref. [61,103]). In fact, the Chagres Sandstone, which conformably overlays the Late Miocene Gatún Formation, has been dated to be at least as old as the Late Miocene[69] (see also ref.[104]). On the other hand, the only extended marine deposits that provide evidence of an interoceanic communication via the Canal Basin is the Early Miocene “La Boca Formation” (more recently re-interpreted as being the lower part of the Culebra Formation[104]). There is, however,

certain other geological evidence suggesting that the Canal Basin might have experienced marine transgression episodes much more recently.

The Canal Basin is broken at the point where the isthmus reaches its lowest topographic elevation, originally ~ 84 m above sea level[88], making it the best location for the construction of the interoceanic Panama Canal and also a possible location for the past exposure of a natural transoceanic seaway. The question is when the current topographical highs in the Canal Basin that currently separate the two oceans emerged. It is known that the Panama Arc began rising around 6 Ma and has continued to rise until the present day. On the other hand, the area maintained a low topography, which was certainly influenced by glacio-eustasy during the Quaternary (e.g. ref.[7]). The detailed chronological sequence of events is not well known, however, because of the complex geological history of the area and the difficulty of making direct geological observations[61].

Within the Canal Zone, the most pronounced expression of low topography in the Canal watershed area is the once-extensive swamp within the broad valley of the Chagres river, which is now covered by the Panama Canal's Gatún lake[105,106]. The valley penetrated to within 25 km of the Pacific Ocean in central Panama, where the Pacific–Caribbean drainage divide descends to one of its lowest elevations in Central America (< 200 m) in the low saddle of the Culebra Cut (also known as the Gaillard Cut) along the Panama Canal[100]. The saddle of the Culebra Cut marks the southern boundary of the Río Chagres basin, the geomorphology of which is the result of four continent-shaping movements that followed the cessation of intense volcanic activity in the Early Miocene and resulted in the erosive and depositional intervals that created the present day land mass[105,107]. During the first movement, the central portion of the isthmus was elevated above the coastal lines, developing the present morphology of the Central and Pacific portions of the isthmus. The second movement elevated the terrain to more than 90 m in the Atlantic area of the isthmus. Slow settling of the land surface characterised the third movement, during which the lower parts of the isthmus were overtaken by the sea, as evidenced by the layers of marine deposits with strictly fluvial beds in the "Atlantic mud" [107]. The Atlantic mud and "Pacific mud" (also known also as sludges or more generally as Quaternary deposits) are informally known deposits with similar physical properties and appearance that unconformably overlay the Miocene marine formations of the Canal Basin[61]. The age of the muds is considered to be Holocene to Late Pleistocene[61,103], which is supported by radiochronological estimations[108]. The muds are contained in swamp and stream deposits extending as far inland as Gamboa on the Caribbean side of the Canal Zone and as far as the Miraflores Locks on the Pacific side[61], separated by the saddle of the Culebra Cut. The muds were deposited upon a stream-eroded topography of considerable relief[105], so that any previous marine deposits in the area were eroded and lost. From this view, the uplift of the area around the saddle of the Culebra Cut might correspond to a more recent age in which there was a marine connection between the Atlantic and Pacific Oceans through the Canal Basin.

Seismic imaging along the Caribbean coast indicates that faults beneath the Limón Bay may be part of a more extensive set of predominantly north and northeast-trending faults, which are also exposed in the

Culebra Cut between Gatún Lake and the Pacific coast[106]. Detailed geologic surveys conducted during the Culebra Cut widening project (1959–1969) revealed over 100 normal, reverse, and strike-slip faults along a single 1.8 km section of the cut. The geologic impression given by the surveys is that the area has been subjected to immense stresses and thoroughly shattered[99]. The faulting in the Canal Zone post-dates Late Miocene strata, and, although the minimum age of displacement is unconstrained, the available data imply a Pliocene or Quaternary age[106]. Indeed, after the cessation of folding in eastern Panama in Plio-Quaternary times[81], the modern tectonics of the Canal Zone are dominated by strike-slip faults, such as the Río Gatún and Pedro Miguel faults (the latter is near and on the right of the Culebra Cut area), which were modelled by uplift and the emergence of central Panama within the last 3 Mya[109]. Geomorphic analysis suggests that the Pedro Miguel fault continues southward offshore into the Pacific Ocean, where Taboga Island may indicate an uplift at a left step on the fault[110]. In particular, on the basis of the slip-rate (4–7 mm/year) and total displacement (~ 5–10 km) along the Pedro Miguel fault, Farris et al.[111] concluded that the fault must be younger than 1–3 Mya.

In conclusion, prominent geomorphic lineaments, topographic breaks, and bends in river courses are all consistent with a young, fault-controlled landscape[100]. Therefore, the available data cannot rule out an age < 1 Mya for the uplift of the topographical high separating the low topographies north and south of the Culebra Cut. Such a high could have constituted a terrestrial barrier to a recent interoceanic marine communication through the low topography of the Panama Canal area.

2.2.4. The Atrato Seaway

The Late Pliocene (~ 3 Mya) reconstruction of Coates and Obando[8] displays another transoceanic seaway through the Atrato and Chucunaque Basins (Fig. 1C), the Atrato Seaway, which was originally proposed by Woodring[112]. Recent stratigraphical research showed, however, that the seaway passing through the Chucunaque Basin was subaerially exposed by 5.6 Mya[81] (see also ref.[113]) and therefore no longer in existence during the Late Pliocene (Figs. 2 & 3). Based on stratigraphic data from a single well in the Atrato Basin (Opogado-1), Coates et al.[81] postulated that the Atrato trough was also subaerially exposed by 4.8 Mya. This age corresponds to the minimum age of the marine deposits at the top of the Munguido Formation in the Opogado-1 well (for detailed biostratigraphy see ref.[114,115]). Coates and Obando[8] and Coates et al.[81] considered the Mongoido Formation to be the last marine formation in the Atrato Basin, but that assessment now appears to be incorrect. The Mongoido Formation is overlain by the Quibdó Formation in wells both north and south of the Opogado-1 well (see ref.[116]: Fig. 21), indicating that the stratigraphic scheme of the Opogado-1 well is not representative of the wider Atrato Basin area and therefore cannot be used to infer general palaeogeographical conclusions about the area.

The Quibdó Formation consists of sandstones and occasional conglomerates including marine faunas, and it is overlain by gravels, sands, and sandstones corresponding to alluvial deposits of the Atrato River[117]. On the basis of a Late Pliocene age for the Quibdó Formation, O'Dea et al.[7] argued that the Atrato Seaway persisted until 3.1 Mya and was overlain thereafter by terrestrial sediments. The minimum

age of the Quibdó Formation is therefore critical for bracketing the age of the exposure of the Atrato Seaway. Although the age of the Quibdó Formation is uncertain, it has been estimated to be Late Pliocene, but also Pliocene to "Quaternary (?)", with a question mark indicating the possibility that the upper boundary falls within the Quaternary (e.g. ref.[117,118]). Other recent stratigraphical schemes display the minimum age of the Quibdó Formation to be ~ 1.8 Mya, albeit also accompanied by a question mark indicating that it might be even younger (e.g. ref.[116]: Fig. 20; ref.[119]: Fig. 17). Stratigraphical schemes in some technical reports show the Quibdó Formation to be Late Pliocene to Middle Pleistocene in age (e.g. ref.[120,121]). The confusion over the age of the Quibdó Formation stems from the purely marine biostratigraphic markers that have been recovered from it so far (see ref.[119]: Fig. 18). These are the benthic foraminifera *Cassidulinella pliocenica* and *Ammonia cf. beccarii* and the planktonic foraminifera *Orbulina cf. universa* (ref.[119]: Fig. 17). While the former is congruent with an age as young as the Late Pliocene[122], the latter two are indicators of an age spanning from the Miocene to recent[123,124]. In the absence of well biostratigraphic markers, geotectonic data provide additional clues regarding the age of the Quibdó Formation.

The importance of the Quibdó Formation for geologists is not mainly stratigraphical but tectonical, as it is considered to describe the emergence of the Serranía de Baudó area, known as the Baudó Event[116,119]. The age (usually referred to as "8–4 Ma ?") and the mechanisms responsible for the Baudó Event remain uncertain, because the available data are insufficient to fully explain the kinematics of the Baudó Range emplacement. In any case, the Baudó Event is believed to have led to the formation of the western margin and closure of the Atrato Basin[125] (Fig. 2). Thus, while the eastern margin of the Atrato Basin records the shallowing of the basin, large deformations toward the western margin in the Baudó Range can be seen as a result of orogenic activity. A noteworthy example of such a dynamic procedure is printed in the Río Murrí section, where the Eocene Salaquí Formation outcrops in fault contact with the Quibdó Formation[116,119]. Late Miocene to Pliocene orogeny in the Northern Andes was likely triggered by the onset of a flat-slab subduction of the Nazca plate underneath the northernmost Andes of Colombia[126]. Thus, a Pliocene age of the Quibdó Formation matches well with the latest Neogene tectonic activity in the Northern Andes. It is also evident, however, that orogeny and uplift in the area occurred since the Early Pleistocene (1.8 Mya) until recently[127]. Therefore, the final configuration of the Serranía de Baudó area and subaerial conditions in the Atrato Seaway could be the results of a more recent procedure that occurred in two steps. In this context, the presence of Quibdó Formation deposits in the Salaquí river area may suggest a past westward marine connection of the Atrato Seaway to the Pacific via the northern Baudó mountain range, which was severed during the Early Pleistocene orogeny.

Northwards, a likely connection between the Atrato Seaway and the Atlantic Ocean passes through the Urabá Basin, which is separated from the Atrato Basin by the Mandé magmatic arc[128]. Detailed surveys of the region showed that the sediments in the Atrato Basin extend into the Urabá Basin[7,128]. In the Urabá Basin, based on the stratigraphic records of the onshore Apartadó-1 and Chigorodó-1 wells, as well as the interpretation of seismic lines, four seismostratigraphic sequences can be defined, ranging from the

Lower Miocene to the Pliocene (?) (ref.[119]: Fig. 22; the question mark indicates that the data are purely biostratigraphic). Even the lithostratigraphic relations among the drilled units that outcrop on the west and east flanks of the basin are uncertain because of a lack of detailed stratigraphic studies in these areas[119]. Nevertheless, the stratigraphic record of the Necoclí-1 well on the right bank of the Urabá Gulf along with the related seismic line transect (see ref.[129]: Fig. 9 & ref.[119]: Fig. 27) reveal the geometry of the Urabá Basin and allow a precise biochonostratigraphic estimation for the facies of the whole foredeep basin. According to this idealised stratigraphic scheme[129], the oldest recorded sedimentary rocks in the Urabá Basin are Lower Miocene deep-water facies, which grade to Pliocene–Early Pleistocene shallow-water siliciclastic deposits and are overlain by more recent alluvial sediments (ref.[129]: Fig. 5c). Therefore, an Early Pleistocene exposure of the Atrato Seaway from the Urabá Basin to the Pacific via a marine trough in the northern Baudó mountain range is congruent with the available data. This seaway is not related to the findings of ref.,[6] because it was located northwards, not southwards, of the Mandé Batholith (see ref.[6]: Fig. 3).

A likely second connection of the Atrato Seaway southwards to the Pacific passes from the adjacent San Juan Basin. There, the Mayorquín Formation can be correlated with the Quibdó Formation on the basis of similarity in age (e.g. ref.[119]). However, the Atrato River Valley to the north and the Pacific Plain to the south were separated by the uplift of the “San Juan Paleohigh,” resulting in the southernmost extension of the “Istmina Deformation Zone.” This uplift was the product of dextral tectonics from the collision of the Panama arch with the Colombia Pacific during the Late Neogene, but the precise age of the event is not well constrained[130].

2.3. Biostratigraphic data

Ancient biotic geodispersals are indicative of dispersal routes and provide proxies of ancient paleogeographic configurations (e.g. ref.[62]). Terrestrial migrations across an isthmus provide evidence that the isthmus was exposed as a land bridge at the time of the migration, whereas the presence of related marine biota on both sides of an isthmus suggests the former presence of a seaway through the isthmus[131]. Evidence from terrestrial biota for the formation of the Isthmus of Panama 1–0.89 Mya has been reviewed under the concept of the Great American Biotic Interchange[17] and, more specifically, the third terrestrial migration event (GABI 3). Evidence of terrestrial migration across the isthmus must be considered indirect evidence, because the observed biogeographic patterns might have been influenced by ecological parameters other than the existence of a land bridge. By contrast, the biogeographic distributions of marine molluscan assemblages constitute direct evidence of the formation of the isthmus. Near the end of the Early Pleistocene, “paciphile” taxa disappeared from the Neogene Caribbean marine molluscan assemblages, which prior to that time had been part of a single bioprovince (the Gatunian Province) that spanned both sides of the isthmus[15,16] (Fig. 4A). Such a recent resemblance in the molluscan assemblages on either side of the isthmus cannot easily be explained if the final emergence of the isthmus occurred 3 Mya. Likewise, the occurrence of the atlantiphile tonnoidean gastropod species *Linatella caudata* in the early-to-mid Pleistocene Armuelles Formation[132] in Pacific

Panama, and that of the paciphile species *Malea ringens* in the Moín Formation of Atlantic Costa Rica (dated 1.9 Mya to < 1 Mya [96]), indicate the existence of shallow-water interoceanic exchange[133] between the Pacific and the Caribbean during the whole Early Pleistocene. Furthermore, the third dispersal event of the Great American Biotic Interchange (GABI 3) between North and South America took place ~ 0.9 Mya[17], resulting in the presence of opossum (*Didelphis*) in North America ~ 0.9 Mya (0.8–1.0 Mya)[17] and that of the jaguarundi *Herpailurus*, the cervid *Paraceros*, the peccary *Pecari*, and the tayassuid *Tayassu* in imprecisely dated Bonaerian beds (Middle Pleistocene, ~ 0.7 Mya) in South America[17,134]. Importantly, the dispersal of *Equus* into South America, which was previously thought to have occurred during the GABI 4 event in the Late Pleistocene (~ 0.125 Mya), was recently reported to have occurred between ~ 0.99 Mya and < 0.76 Mya, an interval that includes the GABI 3[135]. Older records of terrestrial immigrants (e.g. GABI 1 and 2) probably correspond to distinct ephemeral exposures of the isthmus.

2.4. Palaeoceanographic and Stratigraphic Data

Oceanographic models support the hypothesis that the open CAS permitted relatively fresh and cool Pacific water to flow into the North Atlantic, affecting buoyancy by adding freshwater into the Caribbean and weakening the AMOC (e.g. ref.[18]). For example, a narrow (~ 100 km) but deep (~ 2,000 m) transisthmian seaway could exert a profound effect on the global oceanic circulation pattern[18]. The open/close modes of the transisthmian seaway(s) can be traced through changes in ocean salinity and the circulation patterns of ocean surface currents, as well as the circulation of bottom currents and their erosional effect on the ocean floor. Specifically, during periods when the transisthmian seaways were open, low-salinity Pacific waters could penetrate into the high-salinity Caribbean waters, reducing the intensity of the Gulf Stream and the North Atlantic Current on the surface of the Atlantic (Fig. 4) and the NADW on the bottom of the Atlantic.

The dominance of the planktic foraminifera *Globorotalia truncatulinoides* along with enriched $\delta^{13}C_{Nd}$ isotope values in ODP Hole 994C, Blake Ridge, NW Atlantic, have been interpreted to indicate the presence of high-salinity, less-productive surface water in the northern Atlantic derived from an intensified Gulf Stream flow due to closure of the CAS[136]. Such changes have been recorded since 0.9 Mya and thereafter, as well as during earlier intervals[136]. Enhanced Gulf Stream flow is accompanied by increased North Atlantic Deep Water formation (as part of the AMOC). Periods of increased AMOC strength have been linked to increased salinity and warm water transport from the Mediterranean Outflow Water current (MOW)[47]. The increased AMOC strength is marked by depositional hiatuses on the route of the MOW, indicating erosion by bottom currents due to increased volumes circulating into the North Atlantic. Such hiatuses occurred during three periods, the last of which was from 0.9 Mya to 0.7 Mya[47] (Fig.4**D**). Estimation of the variation in Northern Component Water (NCW) overflow, the ancient counterpart of the NADW, also highlights a culmination at 0.9 Mya[46] (Fig.4**C**). Furthermore, the increasing domination of the Caribbean planktic foraminiferal assemblages by the salinity-tolerant species *Globigerinoides ruber* is considered to reflect increased Atlantic surface-water salinity due to cessation of sustained flow between

the Pacific and the Caribbean[9]. The relative abundance of *G. ruber* culminated from 0.9 Mya to 0.6 Mya[3,9] (Fig.4**B**).

Figure 4. Paleobiogeographic and oceanographic data supporting a major step in the restriction of the transisthmian seaways of the Isthmus of Panama, 0.89 Mya and ~ 0.7 Mya. A) Southern Caribbean Neogene biogeographical units[15]. B) Relative abundance of the high-salinity-tolerant planktic foraminiferal species *Globigerinoides ruber*, as a proxy of surface-water salinity[9]. C) Estimation of the variation in Northern Component Water (NCW) overflow[46]. D) Drill core data of IODP Expedition 339 sites, showing major hiatuses caused by increased saline and warm water transport from the Mediterranean Outflow Water current (MOW)[47].

2.5. Paleoclimatic data

Climate models developed since the early 1990s have suggested that closure of the CAS would strengthen the production of warm, high-salinity Gulf Stream water, enhancing heat transport to the North Atlantic and the upper NADW formation in the Labrador and Nordic Seas (ref.[12,137] and references therein). Accordingly, if transisthmian seaways existed in the early Quaternary as remnants of the CAS, their exposure intervals might have been printed in the Quaternary record of changes in Gulf Stream intensity. Because the transisthmian seaways were generally shallow before their final subaerial exposure, Quaternary glacioeustatic sea level changes should have influenced their open/close modes and, thus, the strengths of the Gulf Stream and the North Atlantic Current (Fig. 5). By this way, during glacial stages, sea level falls should have strengthened the Gulf Stream and the North Atlantic Current, increasing ocean surface temperature and transferring heat northwards, contra to the low temperatures that generally prevail during glacial stages. Thus, increased temperatures in North Atlantic surface waters during glacial stages might correspond to intervals of temporary closure and/or essential restriction of the transisthmian seaways. In **Supplementary Fig. 2**, proxies of surface temperatures of the Gulf Stream (IODP Site U1313) and the North Atlantic Current (ODP Sites 980 & 982) are correlated with the mean global temperature proxy and show that, indeed, such intervals existed between ~ 1 Mya and 0.6 Mya. Moreover, as the heat transport through the North Atlantic Current is accompanied by humidity transport, it has long been argued[138,139], and was recently shown by coupled ocean–atmosphere general circulation models[140,141,142,143], that closure of the CAS would result in enhanced precipitation over Greenland. Stratigraphical evidence from ODP Site 646 on the continental rise off southern Greenland (58°12.56N, 48°22.15 W)[19] shows that such an event took place in the eye of the glacial maximum of Marine Isotope Stage 22 (MIS22; **Supplementary Fig. 3**). This event is evidenced by increases in pteridophyte and spermatophyte spore and pollen records (**Supplementary Fig. 3E**), respectively, suggesting that south (and probably east) Greenland experienced an unprecedented local climatic optimum characterised by increased vegetation growth. The event lasted ~ 20,000 years, from 0.89 Mya to 0.87 Mya, and was associated with an episodic increase of ~ 4.5°C in SSTs across the track of the North Atlantic Current (**Supplementary Fig. 3**). Two positive SST culminations in the record of ODP Site 980[53] are particularly well matched with two contemporaneous positive peaks in the spermatophyte

pollen record of MIS22 from South Greenland (Fig. 6 **and Supplementary Fig. 3H**), suggesting that the intensification of the North Atlantic Current was among the reasons for the unprecedented climatic optimum in South Greenland.

3. Results

The available phylogeographic data (see the **Materials and Methods**) show the existence of a number of transisthmian geminate marine and coastal species (Category A species; see **Table 1**) with too recent molecular divergence dates (from 1.1 to 0.65 Mya) that are not consistent with even the youngest estimations for the age of the isthmus (1.8 Mya). Instead, the data suggest that the isthmus was not finally and completely formed until 1.1–0.6 Mya. Most of the relevant species are marine species for which there is no way of dispersal to either side of the isthmus other than an exposed transisthmian seaway. In addition to shallow-water species, the presence of deep-sea bivalves (*Abyssogena* and *Bathymodiolus* in **Table 1**) suggests that at least one exposed seaway maintained a deep sill until ~ 1.1 Mya. Aside from the Category A geminate species, **Supplementary Tables 1 and 2** contain bird and plant species (Category B) with molecular divergence dates that suggest allopatric speciation due to the same vicariant event. Moreover, specific phylogeographic data point to the existence of biogeographical barriers to terrestrial dispersals within the Isthmus of Panama that conclusively correspond to the proposed exposures of four distinct seaways (see **Supplementary Table 3** and Fig. 3): the Nicaraguan Seaway, the Barú Seaway, the Canal Seaway, and the Atrato Seaway. Geotectonic evidence does not rule out the possibility of recent (latest Early Pleistocene) exposures of these seaways but rather, in some cases, confirms their existence. This is surprising, given the widespread acceptance of ~ 3 Mya as the age of the final formation of the Panama Isthmus. Contrary to that hypothesis, the available geotectonic data (see the **Materials and Methods**) suggest that the shallowing, temporary subaerial exposure (due to glacioeustatic sea level change), and ultimate permanent closure of the last four seaways across the isthmus was due to tectonic uplift driven by movements of the Cocos Ridge and Nazca Plates in the Early Pleistocene.

In accordance with the phylogeographical and geotectonic data, marine and terrestrial biostratigraphic data suggest that the final formation of the Isthmus of Panama was more recent than previously thought. Specifically, the persistence of common marine faunal elements during the whole Early Pleistocene in a single marine bioprovince covering the Atlantic and Pacific peri-isthmian area (the Gatunian Province)[15,16] (Fig. 4A) supports the hypothesis that communicative transisthmian seaways existed during that period. As the direction of interoceanic seawater exchange was mainly from Pacific to Atlantic, the closure of the transisthmian seaways at the end of the Early Pleistocene explains the strict extinction of paciphilic elements from the Caribbean thereafter[16]. On the other hand, the third terrestrial migration event in the Great American Biotic Interchange[17] (GABI 3) suggests a dispersal of terrestrial biota due to the closure of the transisthmian seaways at the end of the Early Pleistocene (see the **Materials and Methods**).

Various oceanographic models predict that termination of interoceanic seawater exchange through the Panama seaways should result in perturbation of oceanic circulation and physical properties (e.g. ref.[18]). Such physical and sedimentological changes have been identified ~ 0.89 Mya and ~ 0.7 Mya, suggesting major restrictions of the transisthmian seaways around these ages (see **Fig. 4** and the **Materials and Methods**). Furthermore, contemporaneous changes in heat transport to the North Atlantic via the Gulf Stream (Fig. 5) can be shown using variation in the sea surface temperatures (SSTs) as a proxy. Indeed, North Atlantic SSTs during glacial stages were unusually high, in contrast to the contemporaneous low global mean temperatures of deep waters, suggesting a remarkable intensification of the Gulf Stream that is congruent with the restriction of the transisthmian seaways (**Supplementary Fig. 2** and the **Materials and Methods**). The episodic climatic optimum suggested by the culminations of pollen and spore records from South Greenland during the glacial maximum of MIS 22[19] (**Supplementary Fig. 3**) further supports the hypothesis that there was a major restriction of the transisthmian seaway ~ 0.89 Mya. The culminations required a heat source capable of driving an increase in precipitation and plant growth. Deep-sea cores from around the course of the North Atlantic Current, the ocean surface current that conveys the warm Gulf Stream northwards, display episodic increases of ~ 4.5°C in SSTs during the MIS 22 interval, whereas cores within the subpolar gyre do not (**Supplementary Fig. 3**).

4. Discussion

It has long been believed that the Isthmus of Panama formed ~ 3 Mya[7,8,20]. This view has been taken with such certainty that hundreds, or perhaps thousands, of works have based conclusions on that date[1,2]. The main arguments of this view are based on geotectonic data that were first presented 25 years ago[8] and have not been reconsidered in light of more recent findings. The present review of the available geotectonic data (see the **Materials and Methods**) does not support a ~ 3 Mya age for the Isthmus of Panama but instead suggests that the final formation of the isthmus was a much more recent event caused by a rapid tectonic uplift due to movements of the Cocos Ridge and Nazca Plates in the Early to Middle Pleistocene (i.e. within the last one million years), although the precise time of these events are still under investigation.

The relationship between the elevation of the Isthmus of Panama and oceanographic conditions in the Tropical Eastern Pacific suggests that although today the isthmus is one of the most mountainous regions in Central America (with peaks rising over 3000 m), the modern topography of the region is largely a consequence of rapid uplift during the last few hundred thousand years (since the mid-to-late Pleistocene)[21]. At the time of its formation, the Isthmus of Panama maintained a lowland profile and was therefore sensitive to relative sea level changes[7]. In that context, the unusually high North Atlantic SSTs during glacial stages (**Supplementary Fig. 2**) can be explained as a result of Gulf Stream intensifications due to restriction/closure of transisthmian seaways during glacioeustatic sea level falls. The global mean sea level reached its lowest level of the entire Cenozoic interval at 0.89 Mya[22]. There was also an exceptional climate deterioration around that time, known as the “900-Kyr event,” which can be added to the evidence supporting a recent final formation of the Isthmus of Panama. The cause of the 900-Kyr

event is a great mystery[23,24,25]; however, it was recently demonstrated that the event was not orbitally forced but was instead due to a currently undefined feedback perturbation of the Earth's internal climate system[26] (Fig. 7). There are examples of major and permanent changes in phenomenally unrelated terrestrial and marine records around that time, such as the permanent reduction in the loess grain-size rate (> 63 μm particle content) in the Otindag sandy desert in northeast China[28] (Fig. 7C) and the change in the sedimentation rate of the Bering Sea area[27] (MIS24; Fig. 7B). These changes are contemporaneous with geochemical changes in the oceans (Fig. 7), which could only be explained by a major reorganisation of surface and bottom currents. Such a perturbation of the ocean currents could in turn only be achieved through a major palaeogeographical change.

The closure of the Bering Strait due to the major sea level fall 0.89 Mya was previously suggested[27] as a main reason for the 900-Kyr event and, more generally, the mid-Pleistocene Transition (MPT), the age suggested by paleoenvironmental data as the threshold for the transition of glacial/interglacial periodicity from 41-Kyr cycles to quasi-100-Kyr cycles as well as a significant change in glacial behaviour in general [5,25]. However, because the time window for a possible closure of the Bering Strait was short, such a closure cannot explain the long-term procedure of the MPT, which ranged from 1.2 Ma to 0.6 Ma[27]. A longer procedure, such as the restriction of transisthmian seaways due to tectonic uplift driven by Cocos Plate subduction, seems to fit better with the available data.

Recent modelling experiments showed that the open/close modes of a ~ 2,000-m deep and ~ 100-km wide transisthmian seaway could have profound effects on the global ocean mean state and deep-water mass properties and circulation[18]. In particular, the models showed North Atlantic Deep Water (NADW) penetration into the Pacific below a depth of 1,469 m, with 12.8% of total net mass transport occurring below that depth[18]. Thus, the deep sill property of a transisthmian seaway has implications for global changes in deep-water circulation and could be a driver of long-term changes in climate[18]. The geotectonic data presented in the **Materials and Methods** indicate that the only likely transisthmian seaway (among the four proposed here) with such a deep sill property was the Barú Seaway (Fig. 3). At the south end of that seaway, fine-grained turbidite deposits of the upper Burica Member contain faunas indicating a gradual shoaling from an initial depth of 2,000 m to a final depth of 1,400 m in Late Pliocene through Early Pleistocene times, and strata assigned to the lowermost Armuelles Formation (late Early Pleistocene time) contain faunas indicative of water depths between 1,200 m and 1,300 m[29]. By contrast, the shallow-water molluscs in stratigraphically higher exposures of the Armuelles Formation are indicative of shelf deposits[29], indicating that within the deposition interval of the Armuelles Formation, rapid shoaling took place at the end of the Early Pleistocene. On the basis of these data, Corrigan et al.[29] concluded that rapid uplift due to Cocos Plate subduction took place after the Early Pleistocene. More recently, uplift rates of 1–8 m Ka^{-1} were estimated for the Burica Peninsula over the Late Pleistocene[30]. With a mean uplift rate of 4 m Ka^{-1}, it would take only 0.6 Ma for a 2400 m deep Barú Seaway to become subaerially exposed, meaning that such an exposure could have occurred during the MPT phenomenon, which occurred from 1.2 Mya to 0.6 Mya[27]. Furthermore, with a combined uplift and volcanic accretion

rate of 6 m Ka^{-1}, the Barú volcano (3,474 m) could have emerged during the last 0.6 Mya. Accordingly, the Cocos Plate subduction could correspond to a major step in the shallowing of the formally deep-water Barú Seaway, with important implications for interoceanic deep-water interchange. This hypothesis is supported by the Atlantic/Pacific divergence of deep-sea bivalve species from ~ 1.1 Mya to 0.95 Mya (**Table 1**).

Figure 6 shows a detailed view of the interval preceding the 900-Ky event. A glacioeustatic sea level drop that started ~ 950 Kya (stage 1) culminated at ~ 917 Kya (stage 2). This interval probably signals the final shoaling of the Barú Seaway and the establishment of a shallow setting in all four remaining transisthmian seaways (Fig. 3). The culmination at 917 Kya signals the onset of the failed MIS23 deglacial, which is characterised by increased duration of relatively high insolation and increased SSTs in the North Atlantic (stage 3). During stage 4, reduced insolation contributed to the extremely cold MIS22 glacial, which led to a new low record in eustatic sea level. This low stand probably resulted in subaerial exposure of the Bering Strait and temporary interruption of the East Greenland Current, which was previously forced by water flowing through the Bering Strait[31,32]. The interruption of the East Greenland Current reduced the supply of fresh and cold Arctic water into East and South Greenland (stage 5), which, combined with an interval of increased insolation and increased heat transport from the North Atlantic Current due to restriction of the transisthmian seaways, resulted in climate optimisation in South Greenland. The restriction of the transisthmian seaways was intensified by the extreme glacioeustatic sea level fall 0.89 Mya. A glacioeustatic sea level rise (stage 6) then resulted in a temporary opening of the Bering Strait, intensification of the East Greenland Current, cooling of East and South Greenland, and, finally, temporary interruption of the climatic optimum in South Greenland. A subsequent sea level fall (stage 7) brought back the favourable conditions for another climatic optimum in South Greenland, which lasted until the end of the high insolation period. Thus, the unprecedented local climatic optimum in South Greenland, as well as the 900-Ky event, were probably the result of closures of both the Panama transisthmian seaways and the Bering Strait. By contrast, the MPT is a phenomenon exclusively related to the concept of a recent formation of the Isthmus of Panama and has no relation to the open/close modes of the Bering Strait.

Declarations

Acknowledgements

The author thanks Spencer Lucas for reviewing and commenting on the initial (shorter) version of this manuscript. This research was not funded by public, commercial, or not-for-profit grants.

Declaration of competing interest

The author declares no competing interests.

References

1. Bacon, C. D. *et al*. Biological evidence supports an early and complex emergence of the Isthmus of Panama. *PNAS* **112**, 6110–6115 (2015). DOI: https://doi.org/10.1073/pnas.1423853112
2. Lessios, H.A. The great American schism: Divergence of marine organisms after the rise of the Central American Isthmus. *Annu. Rev. Ecol. Evol. Syst.* **39**, 63–91 (2008). DOI: http://dx.doi.org/10.1146/annurev.ecolsys.38.091206.095815
3. Molnar, P. Closing of the Central American Seaway and the Ice Age: A critical review. *Paleoceanography* **23**, PA2201 (2008). https://doi.org/10.1029/2007PA001574
4. Brikiatis, L. A re-evaluation of the basal age in the DSDP hole, at Site 534, Central Atlantic. *Geographical Research Journal* **14**, 59–66 (2017). http://dx.doi.org/10.1016/j.grj.2017.08.005
5. Pindell, J.L., & Kennan, L., 2009, Tectonic evolution of the Gulf of Mexico, Caribbean and northern South America in the mantle reference frame: An update, in James, K.H., Lorente, M.A., and Pindell, J.L., eds., The Origin and Evolution of the Caribbean Plate: Geological Society of London Special Publication 328, p. 1–55.
6. Montes, C. *et al*. Middle Miocene closure of the Central American Seaway. *Science* **348**, 226–229 (2015). DOI: http://dx.doi.org/10.1126/science.aaa2815
7. O'Dea, A. *et al*. Formation of the Isthmus of Panama. *Science Advances* **2**, e1600883 (2016). http://dx.doi.org/10.1126/sciadv.1600883
8. Coates, A.G. & Obando, J.A. The geologic evolution of the Central American Isthmus. In: J. B. C. Jackson, A. F. Budd & A. G. Coates (Eds), Evolution and Environment in Tropical America, (The University of Chicago Press, Chicago) pp. 21–56 (1996).
9. Keller, G., Zenker, C.E. & Stone, S.M. Late Neogene history of the Pacific-Caribbean gateway. *Journal of South American Earth Sciences* **2**, 73–108 (1989). DOI: https://doi.org/10.1016/0895-9811(89)90028-X
10. Schwarzhans, W. & Aguilera, O. Otoliths of the Myctophidae from the Neogene of tropical America. *Palaeo Ichthyologica* **13**, 83–150 (2013). ISBN: 978-3-89937-166-6
11. Schmidt, D. N. The closure history of the Central American seaway: evidence from isotopes and fossils to models and molecules in Williams, M., Haywood, A. M., Gregory, F. J. & Schmidt, D. N. (eds) Deep-Time Perspectives on Climate Change: Marrying the Signal from Computer Models and Biological Proxies. The Micropalaeontological Society, Special Publications. The Geological Society, London, 429–444 (2007). https://doi.org/10.1144/TMS002.19
12. Karas, C. et al. Pliocene oceanic seaways and global climate. Scientific Reports 7, 39842 (2017). https://doi.org/10.1038/srep39842
13. Leigh, E.G, O'Dea, A & Vermeij, G. J. Historical biogeography of the Isthmus of Panama. Biol. Rev. 89, 148-172 (2013). https://doi.org/10.1111/brv.12048

1. Bagley, J.C., Johnson, J.B. (2014). Testing for shared biogeographic history in the lower Central American freshwater fish assemblage using comparative phylogeography: concerted, independent, or multiple evolutionary responses? Ecol Evol. 4, 1686-1705. doi: 10.1002/ece3.1058.

15. Landau, B. M., Vermeij G. J. & Da Silva, C. M. Southern Caribbean Neogene palaeobiogeography revisited. New data from the Pliocene of Cubagua, Venezuela. *Palaeogeogr. Palaeoclimatol. Palaeoecol*. **257**, 445–461 (2008). https://doi.org/10.1016/j.palaeo.2007.10.019
16. Landau, B., Marques Da Silva, C. & Vermaij, G. 2009. Pacific elements in the Caribbean Neogene gastropod fauna: the source-sink model, larval development, disappearance, and faunal units. *Bulletin de la Société Géologique de France* **180**, 343–352 (2009). DOI: https://doi.org/10.2113/gssgfbull.180.4.343
17. Woodburne, M. O. The Great American Biotic Interchange: Dispersals, tectonics, climate, sea level and holding pens. *J. Mammal. Evol*. **17**, 245–264 (2010). http://dx.doi.org/10.1007/s10914-010-9144-8

1. Sentman, L. T., Dunne, J. P., Stouffer, R. J., Krasting, J. P., Toggweiler, J. R., Broccoli, A. J. (2018). The mechanistic role of the Central American Seaway in a GFDL Earth System Model. Part 1: Impacts on global ocean mean state and circulation. Paleoceanography and Paleoclimatology 33, 840–859. https://doi.org/10.1029/2018PA003364

19. De Vernal, A. & Hillaire-Marcel, Claude. Natural variability of Greenland climate, vegetation, and ice volume during the past million years. *Science* **320**, 1622-1625 (2008). http://dx.doi.org/10.1126/science.1153929
20. Keigwin, L. D. Pliocene closing of the Isthmus of Panama, based on biostratigraphic evidence from nearby Pacific Ocean and Caribbean Sea cores. *Geology* **6**, 630–634 (1978). DOI: https://doi.org/10.1130/0091-7613(1978)6<630:PCOTIO>2.0.CO;2
21. O'Dea, A., Hoyos, N., Rodríguez, F., De Gracia, B. & Degracia, C. History of upwelling in the Tropical Eastern Pacific and the paleogeography of the Isthmus of Panama. *Palaeogeography, Palaeoclimatology, Palaeoecology* **348–349**, 59–66 (2012). https://doi.org/10.1016/j.palaeo.2012.06.007
22. Miller, K. G. et al. Cenozoic sea-level and cryospheric evolution from deep-sea geochemical and continental records. *Sci. Adv*. **6**, eaaz1346 (2020). https://doi.org/10.1126/sciadv.aaz1346
23. Clark, P. U. *et al*. The middle Pleistocene transition: Characteristics. mechanisms, and implications for long-term changes in atmospheric PCO_2. *Quaternary Science Reviews* **25**, 3150–3184 (2006). https://doi.org/10.1016/j.quascirev.2006.07.008
24. Maslin, M. A. & Brierley, C. M. The role of orbital forcing in the early middle Pleistocene transition. *Quaternary International* **389**, 47–55 (2015). https://doi.org/10.1016/j.quaint.2015.01.047
25. Ford, H.L. & T.B. Chalk. 2020. The Mid-Pleistocene enigma. *Oceanography* **33**, in press. https://doi.org/10.5670/oceanog.2020.216.

26. Brikiatis, L. Astronomical control of the hydroclimate during the past 1.2 million years. *Geol Earth Mar Sci* **3**, 1–11 (2021).
27. Kender, S., Ravelo, A.C., Worne, S. et al. Closure of the Bering Strait caused Mid-Pleistocene Transition cooling. *Nat Commun* **9**, 5386 (2018). https://doi.org/10.1038/s41467-018-07828-0
28. Zeng, L. *et al.* Provenance of loess deposits and stepwise expansion of the desert environment in NE China since ~1.2 Ma: Evidence from Nd-Sr isotopic composition and grain-size record. *Global and Planetary Change* **185**, 103087 (2020). https://doi.org/10.1016/j.gloplacha.2019.103087
29. Corrigan, J., Mann, P., Ingle, J. C. Forearc response to subduction of the Cocos Ridge, Panama-Costa Rica. Geol. Soc. Am. Bull. 102, 628–652, (1990). https://doi.org/10.1130/0016-7606(1990)102<0628:FRTSOT>2.3.CO;2
30. Leon-Rodriguez, L., 2007. Benthic Foraminiferal Record of the Pleistocene Uplift of the Sedimentary Deposits of the Burica Peninsula (Costa Rica-Panama) as a Result of Cocos Ridge Subduction beneath the Central American Arc. M.S. thesis, Florida International University, Miami, Florida.

1. De Schepper, S., Schreck, M., Beck, K. et al. Early Pliocene onset of modern Nordic Seas circulation related to ocean gateway changes. Nat Commun 6, 8659 (2015). https://doi.org/10.1038/ncomms9659

32. Horikawa, K., Martin, E., Basak, C. et al. Pliocene cooling enhanced by flow of low-salinity Bering Sea water to the Arctic Ocean. Nat Commun 6, 7587 (2015). https://doi.org/10.1038/ncomms8587
33. Galván-Quesada, S., Doadrio, I., Alda, F., Perdices, A., Reina, R. G., García Varela, M., et al. Molecular phylogeny and biogeography of the amphidromous fish genus *Dormitator* Gill 1861 (Teleostei: Eleotridae). *PLoS ONE* **11**, e0153538 (2016). https://doi.org/10.1371/journal.pone.0153538
34. Egana, J. P., Bloom, D. D., Kuo, C.-H., Hammer, M. P., Tongnunui, P., Iglésias, S. P., Sheaves, M., Grudpan, C., Simons, A. M. Phylogenetic analysis of trophic niche evolution reveals a latitudinal herbivory gradient in Clupeoidei (herrings, anchovies, and allies). *Molecular Phylogenetics and Evolution* **124**, 151–161 (2018). https://doi.org/10.1016/j.ympev.2018.03.011
35. Silva, G., Cunha, R.L., Ramos, A. et al. Wandering behaviour prevents inter and intra oceanic speciation in a coastal pelagic fish. *Sci Rep* **7**, 2893 (2017). https://doi.org/10.1038/s41598-017-02945-0
36. Dudoit, A., Iacchei, M., Coleman R. R, Gaither, M.R., Browne, W.E., Bowen, B. W., Toonen, R. J. The little shrimp that could: phylogeography of the circumtropical Stenopus hispidus (Crustacea: Decapoda), reveals divergent Atlantic and Pacific lineages. PeerJ 6, e4409 (2018). https://doi.org/10.7717/peerj.4409
37. Marek, C. 2015. The Emergence of the Isthmus of Panama – a biological perspective – Dissertation zur Erlangung des Doktorgrades der Naturwissenschaftlichen Fachbereiche der Justus-Liebig Universität Gießen.
38. Katz, A. D. The influence of vicariance and dispersal on the diversification and evolution of springtails (collembola). Ph D Dissertation, University of Illinois at Urbana-

Champaign. http://hdl.handle.net/2142/101700

39. LaBella, A. L., Van Dover, C. L., Jollivet, D., Cunningham, C. W. Gene flow between Atlantic and Pacific Ocean basins in three lineages of deep-sea clams (Bivalvia: Vesicomyidae: Pliocardiinae) and subsequent limited gene flow within the Atlantic. Deep-Sea Research II 137, 307–317 (2017). http://dx.doi.org/10.1016/j.dsr2.2016.08.013
40. Miyazaki, J.-I., Martins, L. dO., Fujita, Y., Matsumoto, H., Fujiwara, Y. Evolutionary Process of Deep-Sea Bathymodiolus Mussels. *PLoS ONE* **5**, e10363 (2010). http://dx.doi.org/10.1371/journal.pone.0010363
41. Archer, F.I., Morin, P.A., Hancock-Hanser, B.L., Robertson, K.M., Leslie, M.S., et al. Mitogenomic phylogenetics of fin whales (Balaenoptera physalus spp.): genetic evidence for revision of subspecies. *PLoS ONE* **8**, e63396 (2013). http://dx.doi.org/10.1371/journal.pone.0063396
42. Lynch Alfaro, J. W. et al. Biogeography of squirrel monkeys (genus Saimiri): South-central Amazon origin and rapid pan-Amazonian diversification of a lowland primate. Molecular Phylogenetics and Evolution 82, 436–454 (2015).

1. Steeves, T. E., Anderson, D. J. & Friesen, V. L. The Isthmus of Panama: a major physical barrier to gene flow in a highly mobile pantropical seabird. *J. Evol. Biol.* **18**, 1000–1008 (2005). https://doi.org/10.1111/j.1420-9101.2005.00906.x
2. Ochoa-Zavala, M. et al. Contrasting colonization patterns of black mangrove (Avicennia germinans (L.) L.) gene pools along the Mexican coasts. Journal of Biogeography 46, 884–898 (2019). https://doi.org/10.1111/jbi.13536

45. Montes, C. *et al*. Evidence for middle Eocene and younger land emergence in central Panama: Implications for Isthmus closure. *GSA Bulletin* **124**, 780–799 (2012). https://doi.org/10.1130/B30528.1
46. Poore, H. R., Samworth, R., White, N. J., Jones, S. M. & McCave, I. N. Neogene overflow of Northern Component Water at the Greenland-Scotland Ridge. *Geochem. Geophys. Geosyst.* **7**, Q06010 (2006). https://doi.org/10.1029/2005GC001085
47. Hernández-Molina, F. J. et al. Onset of Mediterranean outflow into the North Atlantic. *Science* **13**, 344, 1244-1250 (2014). https://doi.org/10.1126/science.1251306
48. Batchelor, C.L. *et al*. The configuration of Northern Hemisphere ice sheets through the Quaternary. *Nat Commun* **10**, 3713 (2019). https://doi.org/10.1038/s41467-019-11601-2
49. Schlitzer, R., Ocean Data View, https://odv.awi.de (2018).
50. Lisiecki, L. E. & Raymo, M. E. A Pliocene-Pleistocene stack of 57 globally distributed benthic $d^{18}O$ records. *Paleoceanography* **20**, PA1003 (2005). https://doi.org/10.1029/2004PA001071

1. Herbert, T., Lawrence, K., Tzanova, A. et al. Late Miocene global cooling and the rise of modern ecosystems. *Nature Geosci* **9**, 843–847 (2016). https://doi.org/10.1038/ngeo2813

2. Naafs, B. D. A., Hefter, J., Acton, G., Haug, G. H., Martínez-Garcia, A., Pancost, R., Stein, R. Strengthening of North American dust sources during the late Pliocene (2.7 Ma). *Earth and Planetary Science Letters* **317-318**, 8–19 (2012). https://doi.org/10.1016/j.epsl.2011.11.026

53. Marino, M., Maiorano, P. & Flower, B. P. Calcareous nannofossil changes during the Mid-Pleistocene Revolution: Paleoecologic and paleoceanographic evidence from North Atlantic Site 980/981. *Palaeogeography, Palaeoclimatology, Palaeoecology* **306**, 58-69 (2011). https://doi.org/10.1016/j.palaeo.2011.03.028

1. Farmer, J.R. et al. Deep Atlantic Ocean carbon storage and the rise of 100,000-year glacial cycles. Nature Geoscience 12, 355–360 (2019). https://doi.org/10.1038/s41561-019-0334-6.
2. Hoogakker, B. A. A., Rohling, E. J., Palmer, M. R., Tyrrell, T. & Rothwell, R. G. Underlying causes for long-term global ocean delta C-13 fluctuations over the last 1.20 Myr. *Earth and Planetary Science Letters* **248**, 15-29 (2006). https://doi.org/10.1016/j.epsl.2006.05.007
3. Sosdian, S.M., Rosenthal, Y. & Toggweiler, J.R. Deep Atlantic carbonate ion and $CaCO_3$ compensation during the Ice Ages. *Paeloceanography and Paleoclimatology* **33**, 546-562 (2018). https://doi.org/10.1029/2017PA003312
4. Schmieder, F., von Dobeneck, T. & Bliel, U. The Mid-Pleistocene climate transition as documented in the deep South Atlantic Ocean: Initiation, interim state and terminal event. *Earth Planet. Sci. Lett.* **179**, 539-549 (2000). https://doi.org/10.1016/S0012-821X(00)00143-6
5. Hodell, D.A., Venz, K.A., Charles, C.D. & Ninnemann, U.S. Pleistocene vertical carbon isotope and carbonate gradients in the South Atlantic sector of the Southern Ocean. Geochem. *Geophys. Geosyst.* **4**, 1004 (2003). https://doi.org/10.1029/2002GC000367
6. Laskar, J. et al. A long-term numerical solution for the insolation quantities of the Earth. Astronomy and Astrophysics 428, 261e285 (2004). http://dx.doi.org/10.1051/0004-6361:20041335
7. Rohling, E. J. et al. Sea-level and deep-sea-temperature variability over the past 5.3 million years. *Nature* **508**, 477–482 (2014).

61. Woodring, W. P. Geology and paleontology of Canal Zone and adjoining parts of Panama. United States Geological Survey Professional Paper 306: 1–759 (1957).
62. Brikiatis, L. Late Mesozoic North Atlantic land bridges. *Earth-Science Reviews* **159**, 47-57 (2016). https://doi.org/10.1016/j.earscirev.2016.05.002
63. Morris-Pocock, J. A., Steeves, T. E., Estela, F. A., Anderson, D. J. & Friesen, V. L. Comparative phylogeography of brown (*Sula leucogaster*) and red-footed boobies (*S. sula*): the influence of physical barriers and habitat preference on gene flow in pelagic seabirds. *Molecular Phylogenetics and Evolution* **54**, 883–896 (2010). http://dx.doi.org/10.1016/j.ympev.2009.11.013
64. Van der Stocken, T. et al. A general framework for propagule dispersal in mangroves. *Biological Reviews* **94**, 1547–1575 (2019). https://doi.org/10.1111/brv.12514

65. Knowlton, N. & Weigt, L. A. New dates and new rates for divergence across the Isthmus of Panama. *Proc. R. Soc. Lond. B* **265**, 2257–2263 (1998). https://doi.org/10.1098/rspb.1998.0568

66. Martin, A.P. & Bermingham, E. Regional endemism and cryptic species revealed by molecular and morphological analysis of a widespread species of Neotropical catfish. *Proceedings of the Royal Society B* **267**, 1135–1141 (2000). https://doi.org/10.1098/rspb.2000.1119

1. Loaiza, J. R. et al. Late Pleistocene environmental changes lead to unstable demography and population divergence of *Anopheles albimanus* in the northern Neotropics. *Molecular Phylogenetics and Evolution* **57**, 1341–1346 (2010). https://doi.org/10.1016/j.ympev.2010.09.016

68. Smith, K. E., Van Ekeris, L. A., Okech, B. A., Harvey, W. R. & Linser, P. J. Larval anopheline mosquito recta exhibit a dramatic change in localization patterns of ion transport proteins in response to shifting salinity: a comparison between anopheline and culicine larvae. *The Journal of Experimental Biology* **211**, 3067–3076 (2008). https://doi.org/10.1242/jeb.019299

1. Collins, L.S., Coates, A.G., Berggren, W.A., Aubry, M.P. & Zhang, J. The late Miocene Panama isthmian strait. *Geology* **24**: 687–690. https://doi.org/10.1130/0091-7613(1996)024<0687:TLMPIS>2.3.CO;2
2. Funk, J., Mann, P., McIntosh, K., Stephens, J. Cenozoic tectonics of the Nicaraguan depression, Nicaragua, and Median Trough, El Salvador, based on seismic-reflection profiling and remote-sensing data. *Geol. Soc. Am. Bull.* **121**, 1491–1521 (2009).
3. Andjić, G., Baumgartner-Mora, C., Baumgartner, P.-O., Petrizzo, M. R., 2018. Tectono-stratigraphic response of the Sandino Forearc Basin (N-Costa Rica and W-Nicaragua) to episodes of rough crust and oblique subduction. The Depositional Record 4, 90-132. https://doi.org/10.1002/dep2.40
4. Alonso-Henar, J., Schreurs, G., Martinez-Dıaz, J. J., Alvarez-Gomez, J. A., & Villamor, P. (2015). Neotectonic development of the El Salvador Fault Zone and implications for deformation in the Central America Volcanic Arc: Insights from 4-D analog modelling experiments. Tectonics, 34, 133–151. https://doi.org/10.1002/2014TC003723
5. Lucas, S. G., Garcia, R., Espinoza, E., Alvarado, G. E., De Mendoza, L. H., Vega, E. (2008). The fossil mammals of Nicaragua. New Mexico Museum of Natural History and Science Bulletin 44, 417-429.
6. Stephens, J. H. (2014). Tectonic and depositional history of an active forearc basin, Sandino basin, offshore Nicaragua. PhD thesis, University of Texas, Dallas, 128 pp.
7. Stoppa, L., Kutterolf, S., Rausch, J., Grobety, B., Pettke, T., Wang, K.-L., Hemming, S., 2018. Journal of Volcanology and Geothermal Research 359. 47–67. https://doi.org/10.1016/j.jvolgeores.2018.06.015
8. Swain, F. M. (1966). Bottom Sediments of Lake Nicaragua and Lake Managua, Western Nicaragua. Journal of Sedimentary Research 36, 522-540. https://doi.org/10.1306/74D71500-2B21-11D7-8648000102C1865D
9. Bezerra, T.N.; Decraemer, W.; Eisendle-Flöckner, U.; Hodda, M.; Holovachov, O.; Leduc, D.; Miljutin, D.; Mokievsky, V.; Peña Santiago, R.; Sharma, J.; Smol, N.; Tchesunov, A.; Venekey, V.; Zhao, Z.; Vanreusel,

A. (2021a). Nemys: World Database of Nematodes. Theristus setosus (Bütschli, 1874). Accessed through: World Register of Marine Species at: http://www.marinespecies.org/aphia.php?p=taxdetails&id=153269 on 2021-05-14

10. Bezerra, T.N.; Decraemer, W.; Eisendle-Flöckner, U.; Hodda, M.; Holovachov, O.; Leduc, D.; Miljutin, D.; Mokievsky, V.; Peña Santiago, R.; Sharma, J.; Smol, N.; Tchesunov, A.; Venekey, V.; Zhao, Z.; Vanreusel, A. (2021b). Nemys: World Database of Nematodes. Polygastrophora octobulba Micoletzky, 1930. Accessed through: World Register of Marine Species at: http://www.marinespecies.org/aphia.php?p=taxdetails&id=228186 on 2021-05-14
11. Bezerra, T.N.; Decraemer, W.; Eisendle-Flöckner, U.; Hodda, M.; Holovachov, O.; Leduc, D.; Miljutin, D.; Mokievsky, V.; Peña Santiago, R.; Sharma, J.; Smol, N.; Tchesunov, A.; Venekey, V.; Zhao, Z.; Vanreusel, A. (2021c). Nemys: World Database of Nematodes. Viscosia papillata Chitwood, 1951. Accessed through: World Register of Marine Species at: http://www.marinespecies.org/aphia.php?p=taxdetails&id=228124 on 2021-05-14
12. Barboza, G., Fernández, A., Barrientos, J. & Bottazzi, G. (1997) Costa Rica: petroleum geology of the Caribbean margin. The Leading Edge 16, 1787–1794. https://doi.org/10.1190/1.1437582
13. Coates, A. G., Collins, L. S. Aubry, M., Berggren, W. A. (2004), The geology of the Darien, Panama, and the late Miocene-Pliocene collision of the Panama arc with northwestern South America, GSA Bulletin 116, 1327–1344. https://doi.org/10.1130/B25275.1
14. Mende, A. Sedimente und Architektur der Forearc-und Backarc-Becken von Südost-Costa Rica und Nordwest-Panamá. Profil 19, 1-130 (2001).
15. Brandes, C., Astorga, A., Littke, R., Winsemannn, J., 2008. Basin modelling of the Limón Back-arc Basin (Costa Rica): burial history and temperature evolution of an island arc-related basin-system. Basin Research 20, 119-142. https://doi.org/10.1111/j.1365-2117.2007.00345.x
16. Coates, A. G., Jackson, J. B. C., Collins, L. S., Cronin, T. M., Dowsett, H. J., Bybell, L. M., Jung, P., Obando, J. A. (1992). Closure of the Isthmus of Panama: the near-shore marine record of Costa Rica and western Panama. Geological Society of America Bulletin 104: 814–828. https://doi.org/10.1130/0016-7606(1992)104<0814:COTIOP>2.3.CO;2
17. Escalante, G. 1990. The geology of southern Central America and western Colombia. In G. Dengo and J. E. Case [eds.], The Caribbean region, 201–230. Geological Society of America, Boulder, CO. https://doi.org/10.1130/DNAG-GNA-H.201
18. JICA, 1983. Geological survey of Baja Talamanca Coal Field, in Prefeasibility study report for the Baja Talamanca Coal development project in the Republic of Costa Rica. Japan International Cooperation Agency, Tokyo, Japan. https://openjicareport.jica.go.jp/pdf/10201903_02.pdf
19. Brandes, C., Astorga, A., Winsemann, J., 2009. The Moín High, East Costa Rica: Seamount, laccolith or contractional structure? Journal of South American Earth Sciences 28, 1–13. https://doi.org/10.1016/j.jsames.2009.02.005
20. Savin, S. M., and Douglas, R. G., 1985, Sea level, climate, and the Central American land bridge, in Stehli, F. G., and Webb, S. D., eds., The great American biotic interchange: New York, Plenum Press, p.

303–324. https://doi.org/10.1007/978-1-4684-9181-4_12

21. Kolarsky, R.A., P. Mann, and W. Montero. 1995. Island arc response to shallow subduction of the Cocos Ridge, Costa Rica. In Geologic and tectonic development of the Caribbean plate boundary in southern Central America, ed. P. Mann, 235-262, Geol. Soc. Am. Spec. Pap. 295. https://doi.org/10.1130/SPE295-p235
22. Collins, L.S., Coates, A.G., Jackson, J.B.C., Obando, J.A., 1995. Timing and rates of emergence of the Limon and Bocas del Toro basins: Caribbean effects of Cocos Ridge subduction? In: Mann, P. (Ed.), Geologic and Tectonic Development of the Caribbean Plate Boundary in southern Central America: Geological Society of America, Special paper, 295, pp. 263–289.
23. Morell, K. D., E. Kirby, D. M. Fisher, and M. van Soest (2012), Geomorphic and exhumational response of the Central American Volcanic Arc to Cocos Ridge subduction. *J. Geophys. Res.* **117**, B04409. https://doi.org/10.1029/2011JB008969
24. Morell, K. D. (2015), Late Miocene to recent plate tectonic history of the southern Central America convergent margin. *Geochem. Geophys. Geosyst.***16**, 3362–3382. https://doi.org/10.1002/2015GC005971
25. Abratis, M., and G. Wörner (2001), Ridge collision, slab-window formation, and the flux of Pacific asthenosphere into the Caribbean realm. Geology, 29(2), 127–130. https://doi.org/10.1130/0091-7613(2001)029<0127:RCSWFA>2.0.CO;2
26. Gardner, T. W., Verdonck, D., Pinter, N. M., Slingerland, R., Furlong, K. P., Bullard, T. F., Wells, S. G. Quaternary uplift astride the aseismic Cocos Ridge, Pacific coast, Costa Rica. *Geological Society of America Bulletin* **104**, 219-232 (1992). https://doi.org/10.1130/0016-7606(1992)104<0219:QUATAC>2.3.CO;2
27. Morell, K. D., D. M. Fisher, T. W. Gardner, P. La Femina, D. Davidson, and A. Teletzke. Quaternary outer fore-arc deformation and uplift inboard of the Panama Triple Junction, Burica Peninsula. *J. Geophys. Res.* **116**, B05402 (2011). https://doi.org/10.1029/2010JB007979
28. McNeill, D.F., Coates, A.G., Budd, A.F., Borne, P.F., 2000, Integrated paleontologic and paleomagnetics stratigraphy of the upper Neogene deposits around Limon, Costa Rica: a coastal emergence record of the Central American Isthmus. Geological Society of America, Bulletin 112, 963–981. https://doi.org/10.1130/0016-7606(2000)112<963:IPAPSO>2.0.CO;2
29. McNeill, D. F., Klaus, J. S., O'Connell, L. G., Coates, A. G., Morgan, W. A., 2013. Depositional sequences and stratigraphy of the Colón carbonate platform: Bocas Del Toro Archipelago, Panama. Journal of Sedimentary Research 83, 183–195. https://doi.org/10.2110/jsr.2013.13

98. Coates, A. G., Mcneill, D. F., Aubry, M-P., Berggren, W. A., Collins, L. S. An Introduction to the Geology of the Bocas del Toro Archipelago, Panama. Caribbean Journal of Science 41, 374-391 (2005).
99. Lowrie, A., Stewart, J., Stewart, R.H., VanAndel, T.J., McRaney, L. Location of the eastern boundary of the Cocos plate during the Miocene. *Marine Geology* **45**, 261– 279 (1982). https://doi.org/10.1016/0025-3227(82)90114-1

1. Marshall, J. S. (2007). The geomorphology and physiographic provinces of Central America in: G. Bundschuh & J. Alvarado (Ed.), Central America: Geology, Resources and Hazards (pp. 1-51). Taylor & Francis, London.
2. Buchs, D.M., Irving, D., Coombs, H. et al. Volcanic contribution to emergence of Central Panama in the Early Miocene. Sci Rep 9, 1417 (2019). https://doi.org/10.1038/s41598-018-37790-2
3. Montes, C. & Hoyos, N. 2020. Isthmian bedrock geology: Tilted, bent, and broken. In: Gómez, J. & Mateus–Zabala, D. (editors), The Geology of Colombia, Volume 3 Paleogene –Neogene. Servicio Geológico Colombiano, Publicaciones Geológicas Especiales 37, p. 451–467. Bogotá. https://doi.org/10.32685/pub.esp.37.2019.15

103. Stewart, R. H., Stewart, J. L., Woodring, W. P. Geologic map of the Panama Canal and vicinity, Republic of Panama. USGS Publications Warehouse, 1980. https://doi.org/10.3133/i1232

1. Kirby M.X., Jones, D.S., MacFadden, B.J. Lower Miocene Stratigraphy along the Panama Canal and Its Bearing on the Central American Peninsula. *PLoS ONE* **3**, e2791 (2008). https://doi.org/10.1371/journal.pone.0002791
2. Jones, S. M. (1950). Geology of Gatun Lake and vicinity, Panama. *GSA Bull.* **61**, 893–922. https://doi.org/10.1130/0016-7606(1950)61[893:GOGLAV]2.0.CO;2
3. Pratt T. L., Holmes M., Schweig E. S., Gomberg J., Cowand H. A., 2003. High resolution seismic imaging of faults beneath Limón Bay, northern Panama Canal, Republic of Panama. *Tectonophysics* **368**, 211-227. https://doi.org/10.1016/S0040-1951(03)00159-8
4. URS Holdings, (2007). Environmental Impact Study; Panama Canal Expansion Project - Third Set of Locks. URS Holdings, Inc.: Panama City, Panama.
5. Redwood, S. D. Late Pleistocene to Holocene sea level rise in the Gulf of Panama, Panama, and its influence on early human migration through the Isthmus. *Caribbean Journal of Earth Science* **51**, 15-31 (2020).
6. Rockwell T.K., Bennett R.A., Gath E., Franceschi P., 2010a, Unhinging an indenter: A new tectonic model for the internal deformation of Panama. Tectonics 29, TC4027. https://doi.org/10.1029/2009TC002571
7. Rockwell T, Gath E, González T, Madden C, Verdugo D, Lippincott C, Dawson T, Owen LA, Fuchs M, Cadena A, Williams P, Weldon E, Franceschi P (2010b) Neotectonics and paleoseismicity of the Limón and Pedro Miguel faults in Panamá: earthquake hazard to the Panamá Canal. Bulletin of the Seismological Society of America 100, 3097–3129. https://doi.org/10.1785/0120090342
8. Farris, D.W., Cardona, A., Montes, C., Foster, D., Jaramillo, C. Magmatic evolution of Panama Canal volcanic rocks: A record of arc processes and tectonic change. *PLoS ONE* **12**, e0176010 (2017). https://doi.org/10.1371/journal.pone.0176010
9. Woodring, W. P., 1966. The Panama land bridge as a sea barrier. Proceedings of the American Philosophical Society 110, 425-433.

10. Barat, F., De Lépinay, B.M., Sosson, M., Müller, C., Baumgartner, P.O. & Baumgartner–Mora, C. 2014. Transition from the Farallon Plate subduction to the collision between South and Central America: Geological evolution of the Panama Isthmus. Tectonophysics, 622: 145–167. https://doi.org/10.1016/j.tecto.2014.03.008
11. Duque-Caro, H., 1990a. Neogene stratigraphy, paleoceanography and paleobiogeography in northwest South America and the evolution of the Panama Seaway. Palaeogeography, Palaeoclimatology, Palaeoecology 77, 203–234. https://doi.org/10.1016/0031-0182(90)90178-A
12. Duque-Caro H., 1990b. The Chocó block in the northwestern corner of South America: structural, tectonostratigraphic and paleogeographic implications: Journal of South American Earth Sciences 3, 71-84. https://doi.org/10.1016/0895-9811(90)90019-W
13. Cediel F., Restrepo I., Marín-Cerón M.I., Duque-Caro H., Cuartas C., Mora C., Montenegro G., García E., Tovar D., Muñoz G., (2009), Geology and Hydrocarbon Potential, Atrato and San Juan Basins, Chocó (Panamá) Arc. Tumaco Basin (Pacific Realm), Colombia.
14. Rodríguez, M. S., 2007. Geological framework of the Pacific Coast sedimentary Basins, Western Colombia. Geología Colombiana 32, 47-62.
15. Mojica, J., Briceño, L. A., Vargas, A., 2011. Los Ríos Atrato y San Juan de la región pacífica de Colombia: Han corrido siempre en las direcciones actuales? Conference paper, Congreso Colombiano de Geología, Medellin, Colombia.
16. Cediel, F., Restrepo, I. (2011) Geology and Hydrocarbon Potential, Atrato, San Juan and Urabá Basins. University EAFIT, Medellin, Colombia (Petroleum Geology of Colombia series, Vol. 3, F. Cediel (ed)), 104 p
17. ANH-Servigecol Ltda, 2008. Geología de superficie y geoquímica de rocas y crudos de la subcuenca del San Juan (Chocó). Technical Report, Agencia National de Hidrocarburos. https://www.anh.gov.co/
18. ANH-G2 Seismic, 2010. Informe final programa sísmico Choco - Buenaventura 2d 2006, subcuenca del Río San Juan, Colombia. Technical Report, Agencia National de Hidrocarburos. https://www.anh.gov.co/
19. Loeblich, A. R. Jr., Tappan, H., 1988. Foraminiferal Genera and Their Classification. Springer, Boston, MA. https://doi.org/10.1007/978-1-4899-5760-3
20. Paleobiology Database 1. Search for *Orbulina universa*. Access on March 08, 2021. https://paleobiodb.org/classic/basicTaxonInfo?taxon_no=113298
21. Paleobiology Database 2. Search for *Ammonia*. Access on March 08, 2021. https://paleobiodb.org/classic/basicTaxonInfo?taxon_no=823
22. Redwood S.D. (2019) The Geology of the Panama-Chocó Arc. In: Cediel F., Shaw R.P. (eds) Geology and Tectonics of Northwestern South America. Frontiers in Earth Sciences. Springer, Cham. https://doi.org/10.1007/978-3-319-76132-9_14

126. León, S., Cardona, A., Parra, M., Sobel, E. R., Jaramillo, J. S., Glodny, J., … Pardo-Trujillo, A. (2018). Transition from collisional to subduction-related regimes: An example from Neogene Panama-Nazca-South America interactions. Tectonics, 37, 119–139. https://doi.org/10.1002/2017TC004785

1. Egbue, O., Kellogg, J. N. Pleistocene to present North Andean "escape". *Tectonophysics* **489**, 248–257 (2010). https://doi.org/10.1016/j.tecto.2010.04.021
2. Garzón Varón, F. (2012). Modelamiento estructural de la zona límite entre la microplaca de Panamá y el bloque norandino a partir de la interpretación de imágenes de radar, cartografía geológica, anomalías de campos potenciales y líneas sísmicas. Thesis, Universidad Nacional de Colombia, Bogotá.
3. Flinch, J. F., 2003, Structural evolution of the Sinu-Lower Magdalena area (Northern Colombia), in C. Bartolini, R. T. Buffler, and J. Blickwede, eds., The Circum-Gulf of Mexico and the Caribbean: Hydrocarbon habitats, basin formation, and plate tectonics: AAPG Memoir 79, p. 776–796.
4. Martínez, J. O., Ramos, E. L., 2011. High-resolution seismic stratigraphy of the late Neogene of the central sector of the Colombian Pacific continental shelf: A seismic expression of an active continental margin. Journal of South American Earth Sciences 31, 28-44. https://doi.org/10.1016/j.jsames.2010.09.003

131. Brikiatis, L. An early Pangaean vicariance model for synapsid evolution. *Scientific Reports* **10**, 13091 (2020). https://doi.org/10.1038/s41598-020-70117-8
132. León-Rodríguez, L. & Collins, L. Large paleobathymetric changes indicate rapid Pleistocene tectonic uplift of the pacific margin of western Panama-eastern Costa Rica. *Geological Society of America Annual Meeting, Abstracts with Programs* **37**, 160 (2005). https://gsa.confex.com/gsa/2005AM/webprogram/Paper97080.html
133. Beu, A. G. Neogene tonnoidean gastropods of tropical and South America: contributions to the Dominican Republic and Panama Paleontology Projects and uplift of the Central American isthmus. Bulletins of American Paleontology 377–378, 1–550. Ithaca, N.Y. : Paleontological Research Institution (2010).
134. Cione, A., Gasparini, G., Soibelzon, L. & Tonni, E. P. *The Great American biotic interchange. A South American perspective* (Berlin, Springer Briefs in Earth System Sciences, 2015).
135. MacFadden, B.J. Dispersal of Pleistocene *Equus* (Family Equidae) into South America and calibration of GABI 3 based on evidence from Tarija, Bolivia. *PLoS ONE* **8**, e59277 (2013). http://dx.doi.org/10.1371/journal.pone.0059277
136. Bhaumik, A. K., Gupta, A. K. & Ray, S. Surface and deep-water variability at the Blake Ridge, NW Atlantic during the Plio-Pleistocene is linked to the closing of the Central American Seaway. *Palaeogeography, Palaeoclimatology, Palaeoecology* **399**, 345-351 (2014). https://doi.org/10.1016/j.palaeo.2014.02.001
137. Sepulchre, P. et al. Consequences of shoaling of the Central American Seaway determined from modeling Nd isotopes. *Paleoceanography* **29**, 176–189

(2014). https://doi.org/10.1002/2013PA002501

138. Berggren, W. A. Role of Ocean Gateways in Climatic Change in Climate in Earth History: Studies in Geophysics (Berggren, W. A. & Crowell, C.) pp. 118-125 (Washington, DC: The National Academies Press, 1982). https://doi.org/10.17226/11798
139. Keigwin, L.D. Isotopic paleoceanography of the Caribbean and east Pacific: role of Panama uplift in late Neogene time. Science 217, 350–352 (1982). https://doi.org/10.1126/science.217.4557.350
140. Murdock, T. Q., Weaver, A. J. & Fanning, A. F. Paleoclimatic response of the closing of the Isthmus of Panama in a coupled ocean-atmosphere model. *Geophys. Res. Lett.* **24**, 253–256 (1997). https://doi.org/10.1029/96GL03950
141. Lunt, D. J., P. J. Valdes, A. Haywood, and I. C. Rutt. Closure of the Panama Seaway during the Pliocene: implications for climate and Northern Hemisphere glaciation. *Clim. Dyn.* **30**, 1–18 (2008). https://doi.org/10.1007/s00382-007-0265-6
142. Schneider, B. & Schmittner, A. Simulating the impact of the Panamanian seaway closure on ocean circulation, marine productivity and nutrient cycling. *Earth Planet. Sci. Lett.* **246**, 367–380 (2006). https://doi.org/10.1016/j.epsl.2006.04.028
143. Klocker, A., Prange, M. & Schulz, M. Testing the influence of the Central American Seaway on orbitally forced Northern Hemisphere glaciation. *Geophys. Res. Lett.* **32**, L03703 (2005). https://doi.org/10.1029/2004GL021564

1. Johnson, K. P., Weckstein, J. D. The Central American land bridge as an engine of diversification in New World doves. *J. Biogeogr.* **38**, 1069-1076 (2011). https://doi.org/10.1111/j.1365-2699.2011.02501.x
2. Smith, B.T., Klicka, J. The profound influence of the Late Pliocene Panamanian uplift on the exchange, diversification, and distribution of New World birds. *Ecography* **33**, 333-342 (2010). https://doi.org/10.1111/j.1600-0587.2009.06335.x
3. Ireland, H. E., Kite, G. C., Veitch, N. C., Chase, M. W., Schrire, B., Lavin, M., Linares, J., Pennington, R. T. Biogeographical, ecological and morphological structure in a phylogenetic analysis of *Ateleia* (Swartzieae, Fabaceae) derived from combined molecular, morphological and chemical data. *Botanical Journal of the Linnean Society* **162**, 39–53 (2010). https://doi.org/10.1111/j.1095-8339.2009.01016.x
4. Wagner, N., Silvestro, D., Brie, D., Ibisch, P. L., Zizka, G., Weising, K., Schulte, K. Spatio-temporal evolution of *Fosterella* (Bromeliaceae) in the Central Andean biodiversity hotspot. *J. Biogeogr.* **40**, 869-880 (2012). https://doi.org/10.1111/jbi.12052
5. Schaefer, H., Hechenleitner, P., Santos-Guerra, A., de Sequeira, M. M., Pennington, R. T., Kenicer, G., Carine, M. A. Systematics, biogeography, and character evolution of the legume tribe Fabeae with special focus on the middle-Atlantic island lineages. *BMC Evolutionary Biology* **12**, 250 (2012). https://doi.org/10.1186/1471-2148-12-250

6. Smith, B. T. et al. The drivers of tropical speciation. *Nature* **515**, 406–409 (2014). https://doi.org/10.1038/nature13687
7. Ward, P.S., Branstetter, M.G. The acacia ants revisited: convergent evolution and biogeographic context in an iconic ant/plant mutualism. *Proc. R. Soc. B* **284**, 20162569 (2017). http://dx.doi.org/10.1098/rspb.2016.2569
8. Wang, B., Ding, Z., Liu, W., Pan, J., Li, C., Ge, S., Zhang, D. Polyploid evolution in *Oryza officinalis* complex of the genus *Oryza*. https://doi.org/10.1186/1471-2148-9-250
9. Vargas, O. M., Goldston, B., Grossenbacher, D. L., Kay, K. M. Patterns of speciation are similar across mountainous and lowland regions for a Neotropical plant radiation (Costaceae: Costus). *Evolution* **74**, 2644-2661 (2020). https://doi.org/10.1111/evo.14108
10. Aguilar, C., Miller, M.J., Loaiza, J.R. et al. Tempo and mode of allopatric divergence in the weakly electric fish *Sternopygus dariensis* in the Isthmus of Panama. *Sci Rep* **9**, 18828 (2019). https://doi.org/10.1038/s41598-019-55336-y
11. Jones, C. P. Phylogeography of the Livebearer *Xenophallus umbratilis* (Teleostei: Poeciliidae): Glacial Cycles and Sea Level Change Predict Diversification of a Freshwater Tropical Fish (2007). All Theses and Dissertations. 1565. https://scholarsarchive.byu.edu/etd/1565
12. Bagley, J. C., Alda, F., Breitman, M. F., Bermingham, E., van den Berghe, E. P., Johnson, J. B. Assessing species boundaries using multilocus species delimitation in a morphologically conserved group of neotropical freshwater fishes, the *Poecilia sphenops* species complex (Poeciliidae). *PLoS ONE* **10**, e0121139 (2015). https://doi.org/10.1371/journal.pone.0121139
13. Bagley, J. C. Hickerson, M. J., Johnson, J. B. Testing hypotheses of diversification in Panamanian frogs and freshwater fishes using hierarchical approximate bayesian computation with model averaging. *Diversity* **10**, 120 (2018). https://doi.org/10.3390/d10040120
14. Santos, J. C. Coloma, L. A., Summers, K., Caldwell, J. P., Ree, R., Cannatella, D. C. Amazonian amphibian diversity is primarily derived from Late Miocene Andean lineages. *PLoS Biol* **7**, e1000056. https://doi.org/10.1371/journal.pbio.1000056
15. Mendoza, A. M., Bolívar-García, W., Vázquez-Domínguez, E., Ibáñez, R., Olea, G. P. The role of Central American barriers in shaping the evolutionary history of the northernmost glassfrog, *Hyalinobatrachium fleischmanni* (Anura: Centrolenidae). *PeerJ* **7**, e6115 http://doi.org/10.7717/peerj.6115
16. Crawford, A. J. Huge populations and old species of Costa Rican and Panamanian dirt frogs inferred from mitochondrial and nuclear gene sequences. *Molecular Ecology* **12**, 2525–2540 (2003). https://doi.org/10.1046/j.1365-294X.2003.01910.x
17. Parham, J. F., Papenfuss, T. J., van Dijk, P. P., Wilson, B. S., Marte, C., Schettino, L. R., Simison, W. B. Genetic introgression and hybridization in Antillean freshwater turtles (*Trachemys*) revealed by coalescent analyses of mitochondrial and cloned nuclear markers. *Molecular Phylogenetics and Evolution* **67**, 176–187 (2013). http://dx.doi.org/10.1016/j.ympev.2013.01.004

18. Fritz, U., Stuckas, H., Vargas-Ramírez, M., Hundsdörfer, A. K., Maran, J., Päckert, M. Molecular phylogeny of Central and South American slider turtles: implications for biogeography and systematics (Testudines: Emydidae: *Trachemys*). *J Zool Syst Evol Res* **50**, 125-136 (2012). http://dx.doi.org/10.1111/j.1439-0469.2011.00647.x
19. Castoe, T. A., Daza, J. M., Smith, E. N., Sasa, M. M., Kuch, U., Campbell, J. A., Chippindale, P. T., Parkinson, C. L. Comparative phylogeography of pitvipers suggests a consensus of ancient Middle American highland biogeography. *J. Biogeogr.* **36**, 88–103 (2009). https://doi.org/10.1111/j.1365-2699.2008.01991.x
20. Mauck, W. M., Burns, K. J. Phylogeny, biogeography, and recurrent evolution of divergent bill types in the nectar-stealing flowerpiercers (Thraupini: *Diglossa* and *Diglossopis*). *Biological Journal of the Linnean Society* **98**, 14–28 (2009). https://doi.org/10.1111/j.1095-8312.2009.01278.x
21. Rocha-Méndez, A., Sánchez-González, L.A., González, C. et al. The geography of evolutionary divergence in the highly endemic avifauna from the Sierra Madre del Sur, Mexico. *BMC Evol Biol* **19**, 237 (2019). https://doi.org/10.1186/s12862-019-1564-3
22. Morales-Jimenez, A. L., Cortés-Ortiz, L., Di Fiore, A. Phylogenetic relationships of Mesoamerican spider monkeys (*Ateles geoffroyi*): Molecular evidence suggests the need for a revised taxonomy. *Molecular Phylogenetics and Evolution* **82**, 484–494 (2015). http://dx.doi.org/10.1016/j.ympev.2014.08.025
23. Silvestro, D., Tejedor, M. F. Serrano-Serrano, M. L. Loiseau, O., Rossier, V., Rolland, J., Zizka, A., Höhna, S., Antonelli, A., Salamin, N. Early arrival and climatically-linked geographic expansion of new world monkeys from tiny African ancestors. *Systematic Biology* **68**, 78–92 (2019). https://doi.org/10.1093/sysbio/syy046
24. Perelman P, Johnson WE, Roos C, Seua´nez HN, Horvath JE, et al. A molecular phylogeny of living primates. *PLoS Genet* **7**, e1001342 (2011). https://doi.org/10.1371/journal.pgen.1001342
25. Nigenda-Moralesa, S. F. et al. Phylogeographic and diversification patterns of the white-nosed coati (*Nasua narica*): Evidence for south-to-north colonization of North America. *Molecular Phylogenetics and Evolution* **131**, 149–163 (2019). https://doi.org/10.1016/j.ympev.2018.11.011

169. Hernández-Almeida, I., Sierro, F. J., Cacho, I. & Flores, J. A. Impact of suborbital climate changes in the North Atlantic on ice sheet dynamics at the Mid-Pleistocene Transition. *Paleoceanography* **27**, PA3214 (2012). https://doi.org/10.1029/2011PA002209
170. McClymont, E. L., Rosell-Mele´, A., Haug, G. H. & Lloyd, J. M. Expansion of subarctic water masses in the North Atlantic and Pacific oceans and implications for mid-Pleistocene ice sheet growth. *Paleoceanography* **23**, PA4214 (2008). https://doi.org/10.1029/2008PA001622
171. Naafs, B. D. A., Hefter, J., Ferretti, P., Stein, R. & Haug, G. H. Sea surface temperatures did not control the first occurrence of Hudson Strait Heinrich Events during MIS 16. *Paleoceanography* **26**, PA4201 (2011). https://doi.org/10.1029/2011PA002135
172. Rodrigues, T. *et al.* A 1-Ma record of sea surface temperature and extreme cooling events in the North Atlantic: A perspective from the Iberian Margin. *Quaternary Science Reviews* **172**, 118e130

(2017). http://dx.doi.org/10.1016/j.quascirev.2017.07.004

173. Ruddiman, W., Raymo, M., Martinson, D., Clement, B. & Backman, J. Pleistocene evolution: Northern Hemisphere ice sheets and North Atlantic Ocean. *Paleoceanography* **4**, 353–412 (1989). https://doi.org/10.1029/PA004i004p00353

174. Lawrence, K. T., Herbert, T. D., Brown, C. M., Raymo, M. E. & Haywood, A. M. High-amplitude variations in North Atlantic sea surface temperature during the early Pliocene warm period, *Paleoceanography* **24**, PA2218 (2009). https://doi.org/10.1029/2008PA001669

Figures

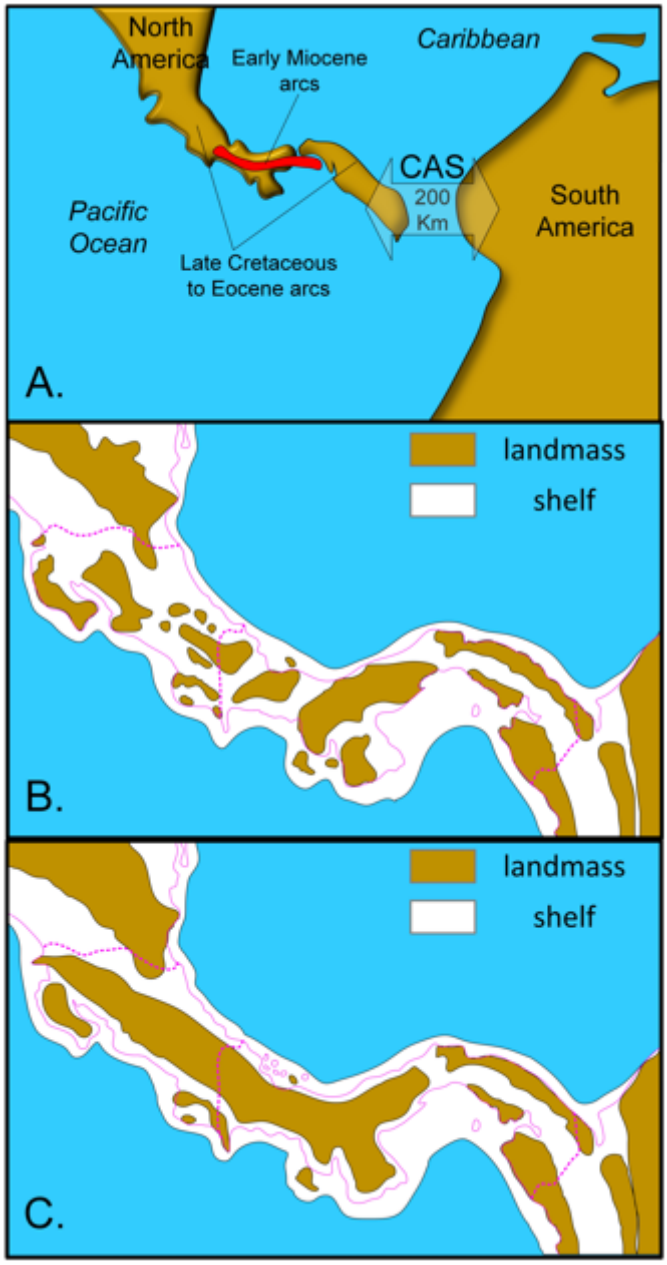

Figure 1

Previous palaeogeographical reconstructions of the Central American Seaway (CAS) and its ruminant straits. A) Early Miocene reconstruction (~20 Mya)45; B) Late Miocene reconstruction (~6–7 Mya)8; C) Latest Pliocene reconstruction (~3 Mya)8.

Figure 2

Modern map of the Isthmus of Panama with marked locations of prominent features mentioned in the text. 1) Nicaraguan Depression; 2) San Carlos Basin; 3) Northern Limón Basin; 4) Southern Limón Basin 5) Tempisque Basin; 6) Burica Peninsula; 7) Barú volcano; 8) Panama Canal; 9) Chucunaque Basin; 10) Urabá Basin; 11) Salaquí river; 12) Serranía de Baudó; 13) Atrato Basin; 14) San Juan Paleohigh; 15) San Juan Basin.

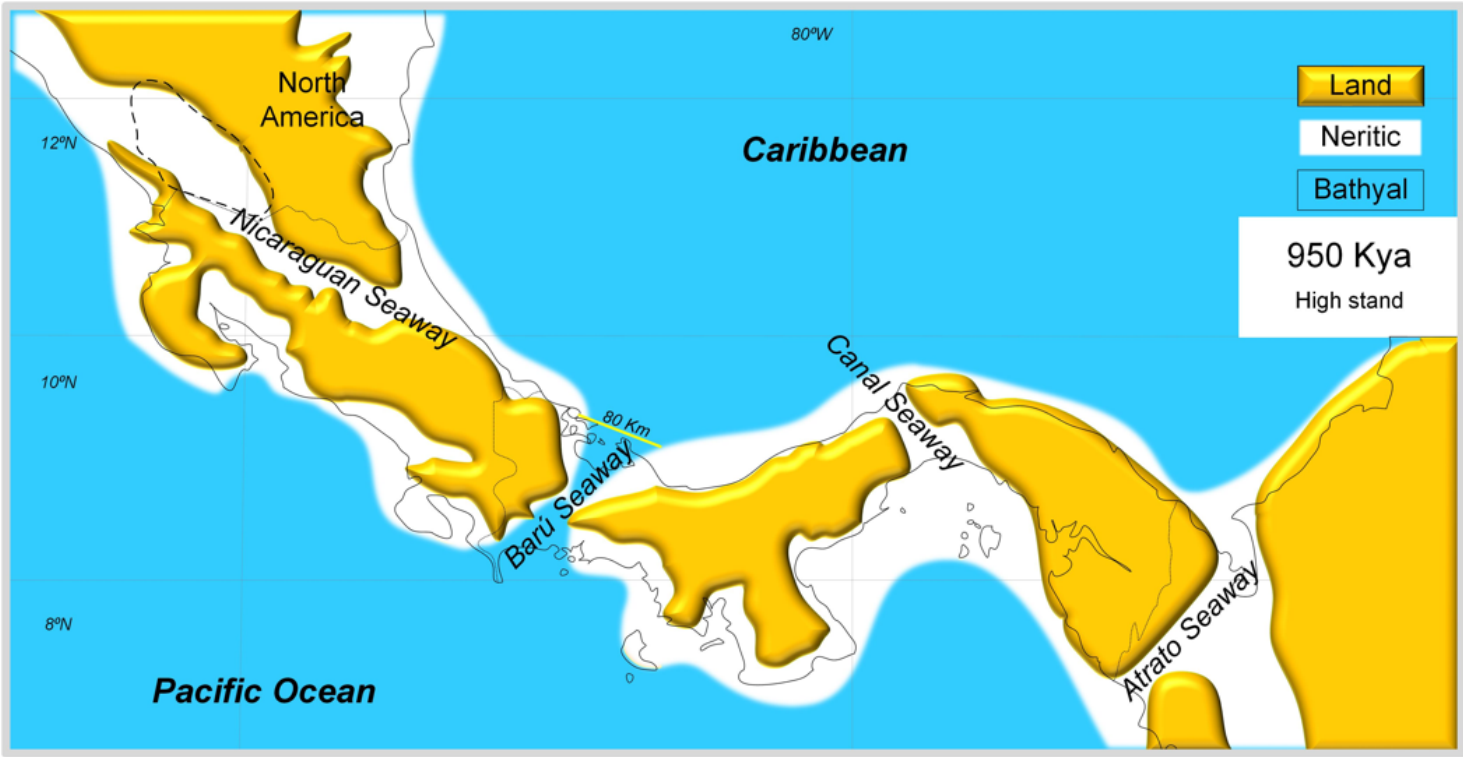

Figure 3

Latest Early Pleistocene palaeogeographical reconstruction of the Isthmus of Panama according to the results of the present study.

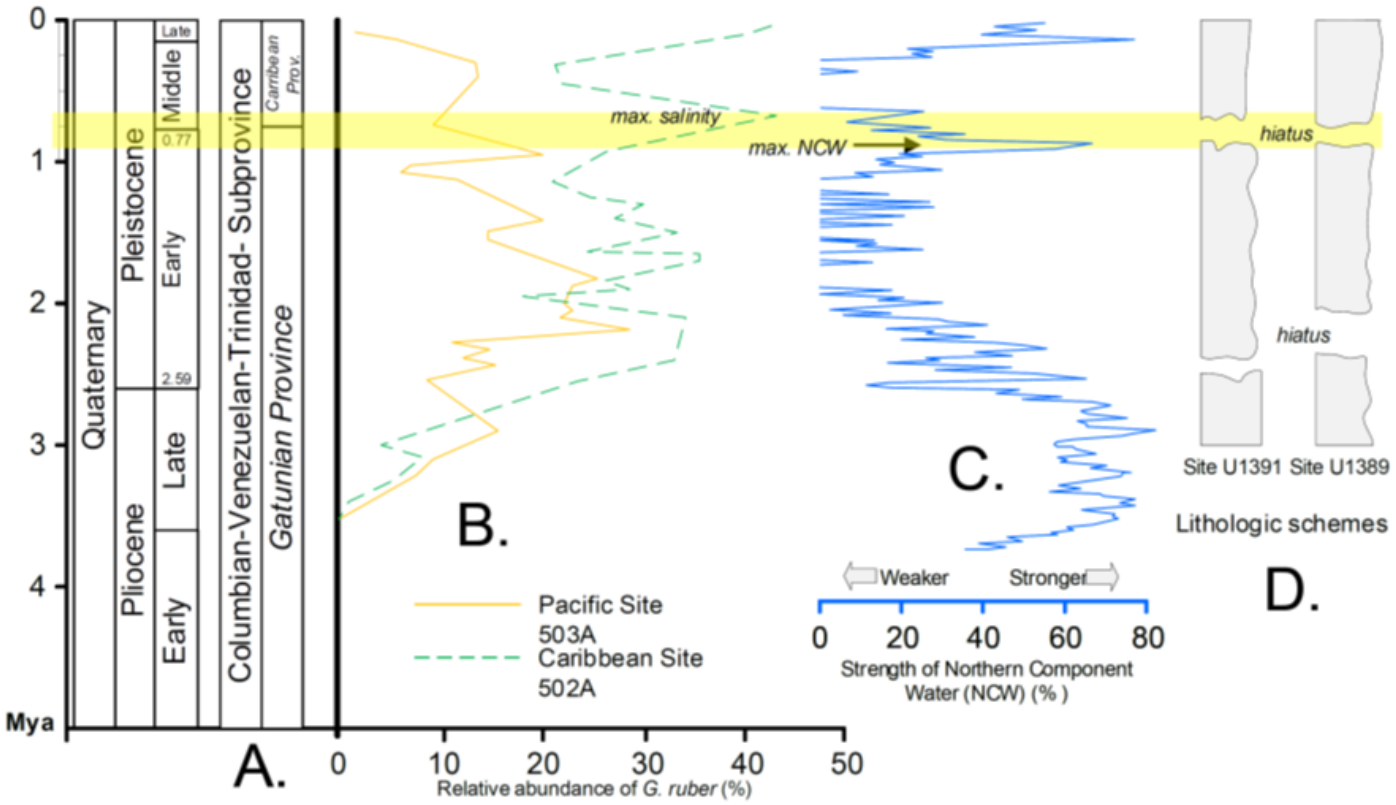

Figure 4

Paleobiogeographic and oceanographic data supporting a major step in the restriction of the transisthmian seaways of the Isthmus of Panama, 0.89 Mya and ~0.7 Mya. A) Southern Caribbean Neogene biogeographical units15. B) Relative abundance of the high-salinity-tolerant planktic foraminiferal species Globigerinoides ruber, as a proxy of surface-water salinity9. C) Estimation of the variation in Northern Component Water (NCW) overflow46. D) Drill core data of IODP Expedition 339 sites, showing major hiatuses caused by increased saline and warm water transport from the Mediterranean Outflow Water current (MOW)47.

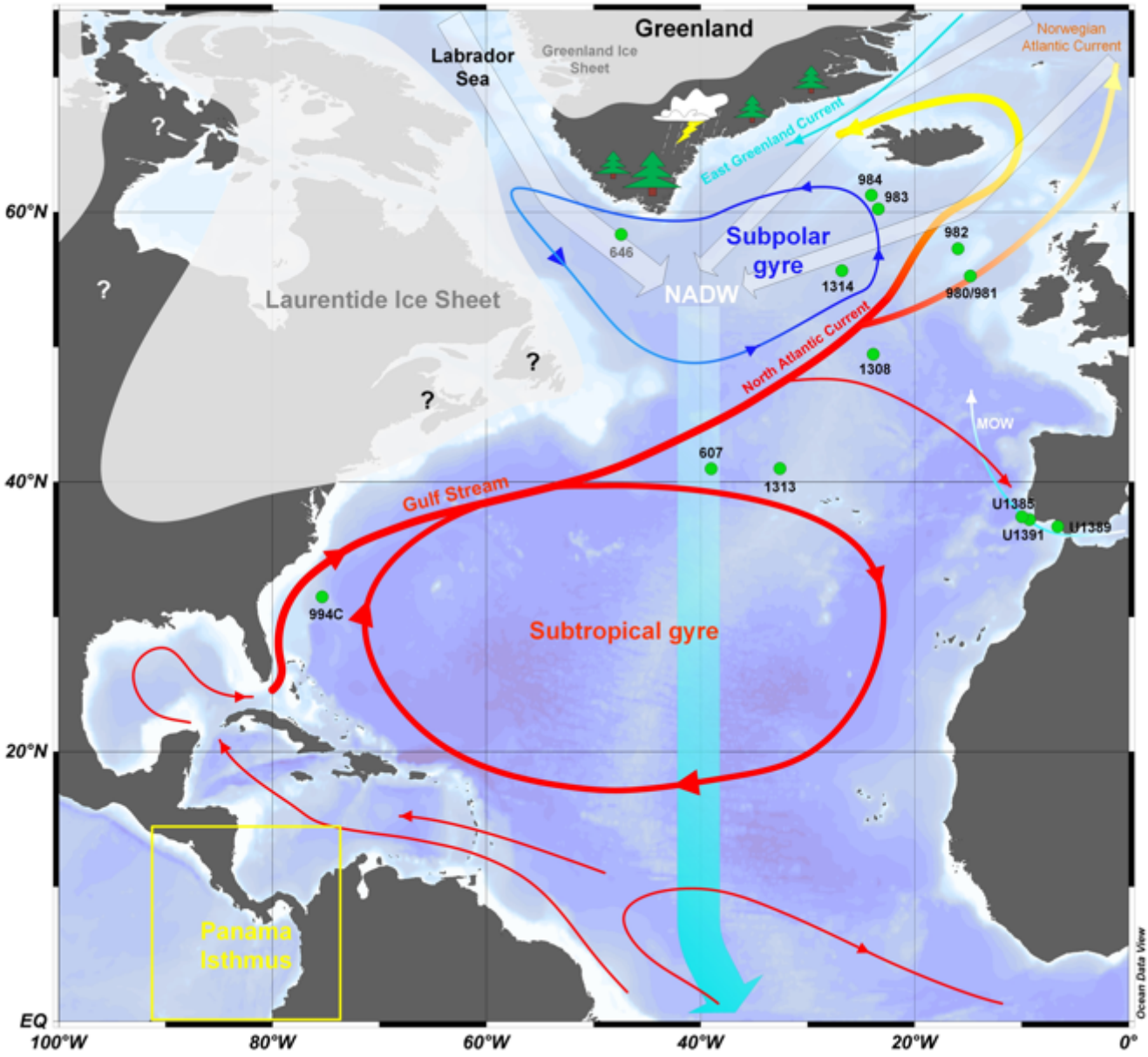

Figure 5

Potential configuration of North Atlantic surface currents during the unprecedented Greenland “greening” at the glacial maximum of MIS 22 due to a major episode in the restriction of the transisthmian seaways and the shutdown of the East Greenland Current 0.89 Mya. Green circles mark the positions of ODP and

IODP sites mentioned in the text and graphs. Hypothesised reconstructions of ice-sheet extent based on ref.48. Map designed using Ocean Data View software49.

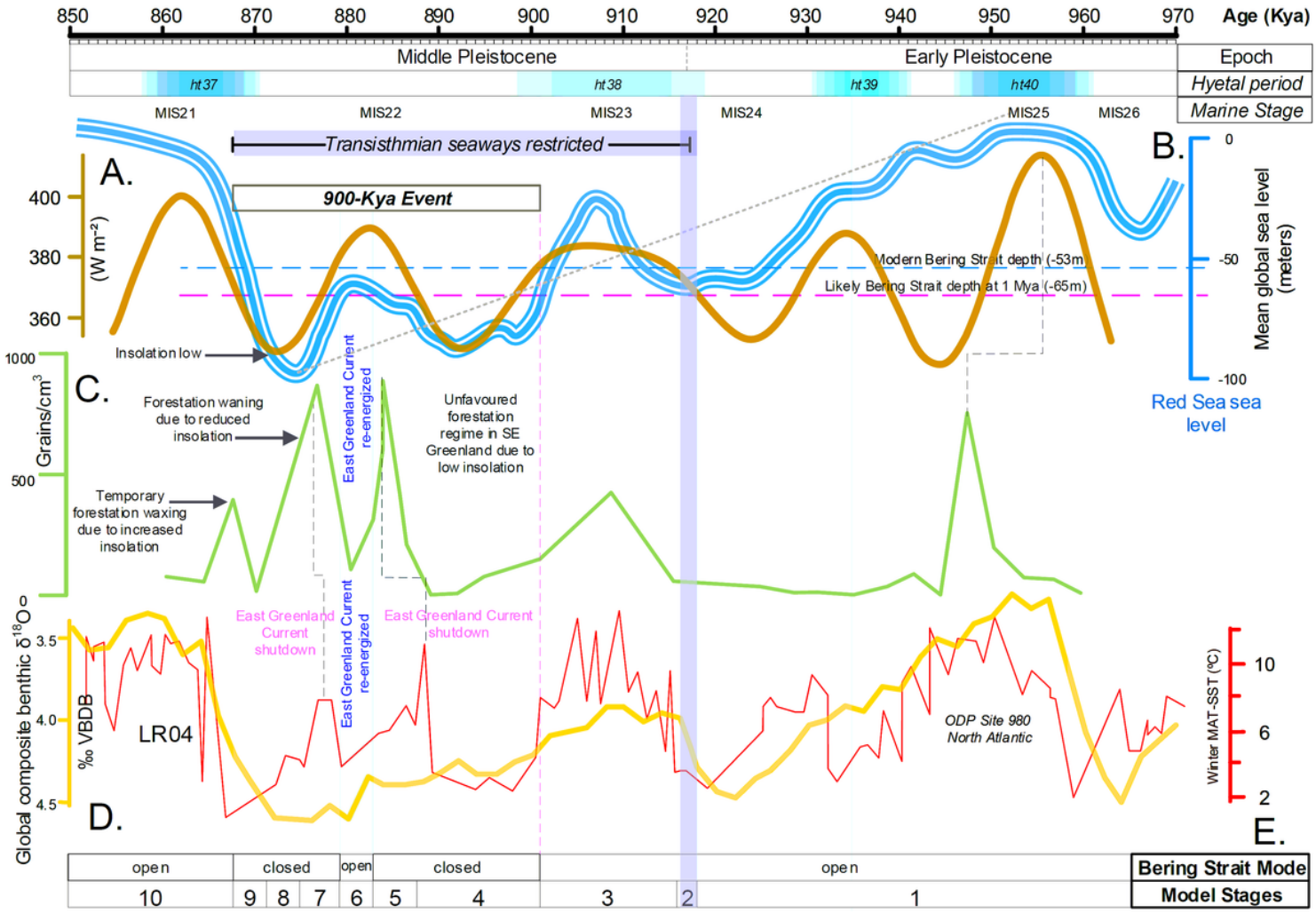

Figure 6

A closer look at the paleoenvironmental parameters that are probably related to the climate perturbation of the 900-Kyr event across the Early-Middle Pleistocene Transition. A) Insolation oscillations at 65°N high latitude59. B) Mean global sea level fluctuation60. C) Pollen content of spermatophytes as an independent proxy of vegetation and forested episodes in South Greenland19. D) Stack of 57 globally distributed benthic δ18O records (palaeotemperature proxy)50. E) Sea surface temperatures (SSTs) from ODP Site 98053. Hyetal spectrum according to ref.26.

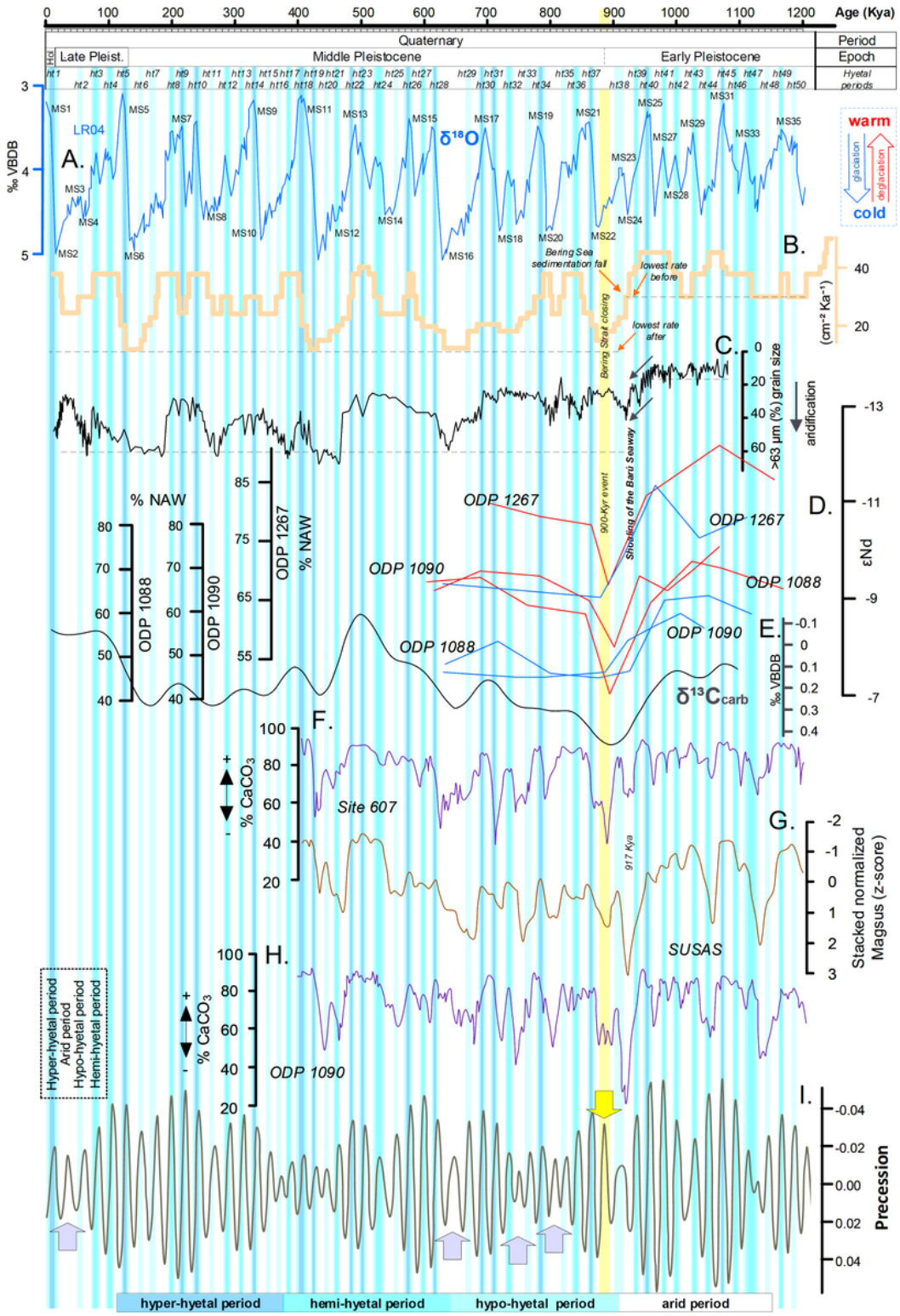

Figure 7

Strict sedimentological and geochemical changes across the Early to Middle Pleistocene Transition. A) Stack of 57 globally distributed benthic δ18O records (palaeotemperature proxy)50. B) Sedimentation rate at the Bering Sea shelf (North Pacific)27. C) Loess grain-size rate (>63 μm particle content) in the Otindag sandy desert, north eastern China28. D) Comparison of planktic foraminiferal Fe-Mn oxide coating εNd from South Atlantic sites 1267, 1088, and 1090 and percent calculated North Atlantic Water

(modified from Supplementary Figure 1 of ref.54). E) Stacked and smoothed carbonate carbon isotope ($\delta^{13}C_{carb}$) from benthic foraminifera of the global ocean55. F) DSDP Site 607 %CaCO356. G) SUSAS South Atlantic magnetic susceptibility stack57. H) South Atlantic DSDP Site 1090 %CaCO358. I) Precessional oscillations of the Earth's rotational axis59. Hyetal spectrum according to ref.26. The grey arrows note that precession minima correspond to hypo-hyetal and/or arid periods only during periods of eccentricity minima26. The only exception to that rule occurs at ~880 kyr (marked by a yellow arrow and a yellow vertical bar) and coincides with the 900-Kyr event26.

Supplementary Files

This is a list of supplementary files associated with this preprint. Click to download.

- Supplementaryinformation.pdf